https://doi.org/10.1186/s40068-020-00216-y

Environmental Systems Research

RESEARCH

Open Access

Spatiotemporal variability and trends of rainfall and its association with Pacific Ocean Sea surface temperature in West Harerge Zone, Eastern Ethiopia

Getachew Bayable[1*], Gedamu Amare[2], Getnet Alemu[3] and Temesgen Gashaw[1]

Abstract

Background: Rainfall variability exceedingly affects agriculture in Ethiopia, particularly in the eastern region where rainfall is relatively scarce. Hence, understanding the spatiotemporal variability of rainfall is indispensable for planning mitigation measures during high and low rainfall seasons. This study examined the spatiotemporal variability and trends of rainfall in the West Harerge Zone, eastern Ethiopia.

Method: The coefficient of variation (CV) and standardized anomaly index (SAI) were used to analyze rainfall variability while Mann-Kendall (MK) trend test and Sen's slop estimator were employed to examine the trend and magnitude of the rainfall changes, respectively. The association between rainfall and Pacific Ocean Sea Surface Temperature (SST) was also evaluated by Pearson correlation coefficient (r).

Results: The annual rainfall CV during 1983–2019 periods is between 12 and 19.36% while the seasonal rainfall CV extends from 15–28.49%, 24–35.58%, and 38–75.9% for average *Kiremt* (June–September), *Belg* (February–May), and *Bega* (October–January) seasons, respectively (1983–2019). On the monthly basis, the trends of rainfall decreased in all months except in July, October, and November. However, the trends were not statistically significant ($\alpha = 0.05$), unlike in November. On a seasonal basis, the trends of mean *Kiremt* and *Belg* seasons rainfall decreased while it increased in *Bega* season although it is not statistically significant. Moreover, the annual rainfall showed a non-significant decreasing trend. The findings also revealed that the correlation between rainfall and Pacific Ocean SST was negative for *Kiremt* while positive for *Belg* and *Bega* seasons. Besides, annual rainfall and Pacific Ocean SST was negatively correlated.

Conclusions: High spatial and temporal rainfall variability was observed at the monthly, seasonal, and annual time scales. Seasonal rainfall has high inter-annual variability in the dry season (*Bega*) than other seasons. The trends in rainfall were decreased in most of the months. Besides, the trend of rainfall decreased in the annual, *Belg* and *Kiremt* season while increased in the *Bega* season. The study also indicated that the occurrence of droughts in the study area was associated with ENSO events like most other parts of Ethiopia and East Africa.

Keywords: CHIRPS, MK trend test, Rainfall variability, SST

Introduction

In recent decades, climate change and variability generate a significant impact on the environment, society, and economy globally (IPCC 2007; Tierney et al. 2013; Birkmann and Mechler 2015; Wang et al. 2018). Anthropogenic and natural factors are responsible for

*Correspondence: bayable.geta@gmail.com
[1] Department of Natural Resource Management, College of Agriculture and Environmental Science, Bahir Dar University, Bahir Dar, Ethiopia
Full list of author information is available at the end of the article

the devastating climate change through the emission of greenhouse gases (GHGs). As a result, climate change is becoming a serious problem to ensure sustainable development. Rainfall is one of the major climatic variables that affect both the spatial and temporal patterns of water availability for agriculture, industry, food security, hydropower water supply, and energy balance (Zhang et al. 2011; Pal et al. 2017; Ayehu et al. 2018; Weldegerima et al. 2018). In many African countries, more than 85% of the population is engaged in rain-fed agriculture (Diro et al. 2011; Mulugeta et al. 2019). Due to this, they are exceedingly susceptible to anomalously high and/or low rainfall amounts (Anyah and Qiu 2012; IPCC 2018). The impact of climate change on the developing countries is higher than developed countries since their adaptive capacity is very low (IPCC 2014).

In East Africa, rainfall is characterized by its inter-annual variability, which has contributed to the shocking droughts and floods; affecting the lives of many people (Cheung et al. 2008; Viste et al. 2013; Mekasha et al. 2014; Tierney et al. 2015). This situation increases the number of people who demand shelter and food aid from time to time. Due to this, climate change and/or climate variability have become the major global agenda which needs collective solutions to reduce its adverse impacts. Ethiopia is known for its high rainfall variability across space and time due to geographical location and topographic complexity (Mengistu et al. 2014; Worku 2015). In Ethiopia, spatial variations can be characterized by the rainfall seasonal cycle, amount, onset, and cessation times, and length of growing season (Segele and Lamb 2005). Moreover, rainfall can be temporally varied from days to decades in terms of the direction and magnitude of rainfall trends over regions and seasons (Jury and Funk 2013; Worku et al. 2019). Reliable and appropriate seasonal rainfall trend analysis and rainfall forecasts are crucial for the mitigation of rainfall related disasters (Diro et al. 2011).

Analyses of spatiotemporal variability and trend of rainfall is vital for water resource management, agricultural production, and climate change mitigation measures (Ayalew et al. 2012; Zhao et al. 2015). More specifically, the occurrence of floods and droughts which are disastrous to the lives of many humans and properties could be reduced by applying early warning systems based on the information on annual, seasonal and monthly trends of rainfall. For this purpose, it requires consistent and spatially well-distributed long-term meteorological station records. The distributions of meteorological stations in developing countries are scarce, unevenly distributed, have poor data quality and data discontinuities (Katsanos et al. 2016; Kimani et al. 2017; Fenta et al. 2018). These are also the limitations of meteorological stations in West Harerge Zone. To overcome these problems, long-term satellite-based rainfall estimates have become vital sources of rainfall data for sparse regions (Ayehu et al. 2018; Dinku et al. 2018; Fenta et al. 2018; Alemu and Bawoke 2019). Long-term satellite-based rainfall estimate can be used in complement or replace meteorological station data to get improved results.

Currently, understanding the spatial-seasonal variations of rainfall and its association with Pacific Ocean SST is very crucial to produce reliable weather and climate forecasts for users (Degefu et al. 2017). Previous studies showed that El Niño/Southern Oscillation (ENSO) has a great influence on the inter-annual rainfall variability in Ethiopia. In 2015, the northern and central parts of Ethiopia were extremely affected by El Niño and the worst drought was occurred. During El Niño (La Niña), precipitation in equatorial east Africa might be positively or negatively affected by easterly (westerly) wind anomalies (Ratnam et al. 2014). ENSO is the inter-annual fluctuation of the atmosphere-ocean system in the equatorial Pacific and it has three phases: warm (El Niño), cold (La Niña), and neutral (Chen et al. 2014; Yu et al. 2015; FAO 2019). Neutral conditions occur when neither El Niño nor La Niña is present. El Niño is a recurrent global atmospheric oceanic phenomenon associated with an increase in SST in the central tropical Pacific Ocean. It boosts the risk of heavy rainfall and flooding in some parts of the world and the risk of drought in some parts (FAO 2019). The SST of the tropical Pacific shows a discrepancy both spatially and temporally (Philip 2018) and a very high correlation exists between precipitation and SST (Wu et al. 2008; Chen et al. 2014).

Several studies (Mohammed et al. 2018; Moloro 2018; Weldegerima et al. 2018; Abegaz and Mekoya 2020; Geremew et al. 2020) have been conducted on the spatiotemporal variability and trends of rainfall in Ethiopia. However, there are limitations in West Harerge Zone. Most of the previous studies were conducted based on meteorological stations rainfall data in eastern Ethiopia. In contrast, meteorological rainfall data and satellite-based rainfall estimates were used in the present study. West Harerge Zone is one of the most droughts prone areas of Ethiopia due to variations of rainfall intensity which can be linked to ENSO. Hence, the objective of this study was to investigate the spatiotemporal variability and trends of rainfall and its association with Pacific Ocean SST in West Harerge Zone of eastern Ethiopia. The findings from this study would be vital for future planning and development measures such as flood control and protection; drought monitoring and early warning systems.

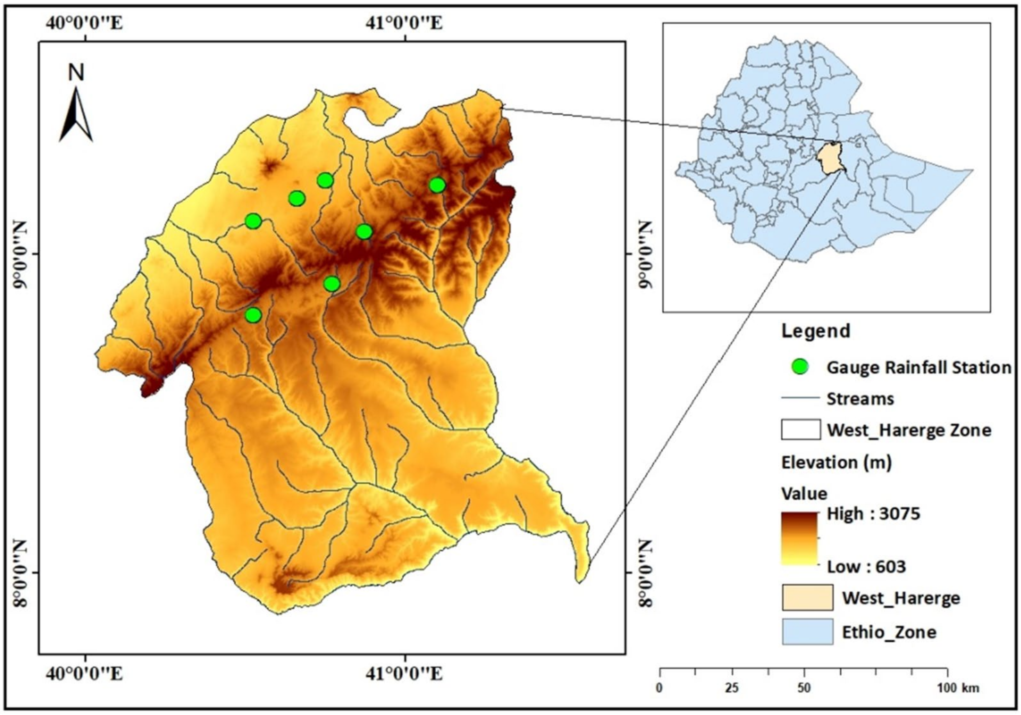

Fig. 1 Location map of the study area

Materials and methods

Description of the study area

The study area, West Harerge Zone, is located in eastern Ethiopia, approximately between 7° 51′– 9° 28′ N and 40° 01′–41° 34′ E (Fig. 1). It covers a total area of 1689497.6 ha of land (Wondosen 2017) and its elevation ranges from 603 to 3075 m a.s.l (Fig. 1). Based on the traditional agroecological classifications of Ethiopia, the study area is categorized into three zones. These are tropical (500–1500 m), sub-tropical (1500–2300 m), and temperate (2300–3200 m) (OWWDSE 2010). There are two rainy seasons in this area, the main rainy season (*Kiremt)* spans from June to September and the short rainy season (*Belg)* extends from February to May. It has the mean monthly rainfall and an average temperature of 67.8 mm and 17.5 to 27.5 °C, respectively (MOA 2000).

Data types and sources

SST and rainfall data were obtained from different sources. Time series monthly Pacific Ocean SST data (1984–2018) in the NINO 3.4 region were downloaded from the National Oceanic and Atmospheric Administration (NOAA) satellite mission website (http://www.cgd.ucar.edu/cas/catalog/climind/TNI_N34/index.html). The NINO 3.4 index mean SST was calculated by taking the spatial average SST within the NINO 3.4 region, which extends from 5° N to 5° S latitude and from 120° W to 170° W longitude (in the Pacific Ocean) (Loua et al. 2019; Yin et al. 2020). According to Babu (2009) and Zaroug (2010), NINO 3.4 SST data has characteristics of both NINO 3 and NINO 4. Accordingly, the Pacific Ocean SST of the NINO 3.4 region was used in this study.

Rainfall data were collected from remote sensing satellite estimates and from the National Meteorological Service Agency (NMSA) of Ethiopia. Most rainfall data from in-situ meteorological stations had short period records and a large percentage of missing data problems (1983–2019). Moreover, the spatial distributions of stations were scarce and not evenly dispersed in the study area. In such cases, Climate Hazards Group Infra-Red Precipitation with Stations (CHIRPS) satellite rainfall data (https://data.chc.ucsb.edu/products/CHIRPS-2.0/) are a vital source of rainfall data (Asfaw et al. 2018; Dinku et al. 2018; Belay et al. 2019). CHIRPS is a quasi-global dataset (covering the area between 50° N and 50° S) available from 1981 to present-day at 0.05° spatial resolution (~ 5.3 km) and it is produced using multiple data sources (Funk et al. 2015). In-situ meteorological station data for Asebe Teferi, Hirna, Bedesa, Gelemso, Meiso, Asebot, and Kora from the NMSA of Ethiopia were used (Table 1) as a reference to evaluate the accuracy of the CHIRPS satellite rainfall product in West Harerge Zone. Missing values were handled by taking the average of the preceding and succeeding months for monthly missed

Table 1 Characteristics of in-situ meteorological stations and percentage of missing data

Station name	Longitude (E)	Latitude (N)	Elevation (m)	Period	Missing data (%)
Asebe Teferi	40.87°	9.07°	1792	1987–2017	16.13
Asebot	40.66°	9.18°	1420	1996–2017	13.63
Bedessa	40.77°	8.91°	1703	1995–2017	4.35
Gelemso	40.53°	8.81°	1739	1987–2017	19.35
Hirna	41.10°	9.22°	1822	1987–2015	10.34
Kora	40.53°	9.10°	1239	1987–2016	16.66
Meiso	40.75°	9.23°	1400	1987–2016	6.66

Table 2 Statistical indicators, equation, range, and best value used in the study

Statistic	Equation	Range	Unit	Best value
Pearson Correlation Coefficient (r)	$r=\frac{\sum_{i=1}^{n}(Gi-\bar{G})(Si-\bar{S})}{\sqrt{\sum_{i=1}^{n}(Gi-\bar{G})^2\sum_{i=1}^{n}(Si-\bar{S})^2}}$	− 1 to 1	None	1
Nash–Sutcliff efficacy Coefficient (NSE)	$NSE = 1-\frac{\sum_{i=1}^{n}(Gi-Si)^2}{\sum_{i=1}^{n}(Gi-\bar{G})^2}$	− ∞ to 1	None	1
Root Mean Square Error (RMSE)	$RMSE = \frac{\sqrt{\sum_{i=1}^{n}(Si-Gi)^2}}{n}$	0 to ∞	mm	0
Mean Absolute Error (MAE)	$MAE = \frac{1}{n}\sum_{i=1}^{n}\lvert Si-Gi\rvert$	0 to ∞	mm	0
Mean Bias Error (MBE)	$MBE = \frac{1}{n}\sum_{i=1}^{n}(Si-Gi)$	− ∞ to ∞	mm	0

Where n is the length of the time series, and i is the number of years. Gi and Si are the meteorological gauge rainfall value and CHIRPS rainfall value in the year i, respectively, and $\bar{G}$ and $\bar{S}$ are the mean meteorological gauge rainfall and the mean of CHIRPS rainfall, respectively

data but years with missed data were excluded from analysis in the station data (Traore et al. 2014; Asfaw et al. 2018).

Validation of CHIRPS rainfall data

Satellite-based rainfall estimates provide well timed, repetitive, and cost-effective information at different time scales (Toté et al. 2015; Muthoni et al. 2019). Due to this, satellite-based rainfall products have been substantially used as complements to meteorological station data or by replacing it. However, they show different uncertainties with techniques. These may arise from relative algorithm errors, spatiotemporal sampling errors, and satellite instruments themselves (Fenta et al. 2018; Alemu and Bawoke 2019; Belay et al. 2019). These may affect the accuracy and may result in a significant error when used for different applications. Accordingly, the validation of satellite rainfall data is required at different spatial and temporal scales (Ayehu et al. 2018; Dinku et al. 2018). The CHIRPS data product is developed by the United States Geological Survey (USGS) and the Climate Hazards Group (CHG) at the University of California (Knapp et al. 2011; Funk et al. 2015).

Validation of the CHIRPS satellite rainfall data was performed on the monthly, seasonal, and annual time scales for Asebe Teferi, Asebot, Bedesa, Hirna, Gelemso, Meiso, and Kora locations with the corresponding meteorological gauge station data. The performance of CHIRPS rainfall data was assessed using different statistics (Table 2) (Dinku et al. 2018; Larbi et al. 2018; Goshime et al. 2019). Root mean square error (RMSE) (ranges from 0 to ∞), mean bias error (MBE) (ranges from − ∞ to ∞) and mean absolute error (MAE) (ranges from 0 to ∞) measures the average magnitude of estimation error and the perfect score for these statistics is zero. Positive and negative MBE value indicates an overestimation and underestimation of CHIRPS data products, respectively (Fenta et al. 2018). Based on some previous studies the RMSE values between 0 and 100 mm are indicated as a good level of performance of the CHIRPS rainfall data (Ayehu et al. 2018, Bayissa et al. 2017, Gebremicael et al. 2017, Nogueira et al. 2018).

Pearson Correlation Coefficient (r) measures the strength of the linear relationship between CHIRPS and meteorological station rainfall data (Alemu and Bawoke 2019) and ranges from negative one to positive one, and values greater than 0.5 are considered as acceptable levels of performance. The Nash–Sutcliff efficacy Coefficient (NSE) describes the relative magnitude of the variance of the residuals compared to the variance of the observed values of precipitation (Nash and Sutcliffe 1970) and it ranges from $-\infty$ to 1. The NSE values between zero and one are generally viewed as acceptable levels of performance, whereas values less than zero indicates that the meteorological station is a better estimate, which indicates unacceptable performance, and zero indicates that the meteorological station is as good as the CHIRPS rainfall products.

Spatiotemporal variability and trend analysis of rainfall

The coefficient of variation (CV) and standardized anomaly index (SAI) were computed to analyze the temporal variability of rainfall.

i. Coefficient of Variation (CV)

Spatiotemporal variability of annual, seasonal, and monthly rainfall for each pixel was examined by calculating the coefficient of variation (CV) (Muthoni et al. 2019). CV was computed as:

$$\mathrm{CV}(\%) = \left(\frac{\sigma}{\overline{\mathrm{x}}}\right)100 \tag{1}$$

where CV is the coefficient of variation of rainfall, σ is the standard deviation of rainfall and $\bar{\mathbf{x}}$ is the long-term mean of rainfall.

ii. Standardized Anomaly Index (SAI)

Standardized anomaly index (SAI) was used as a descriptor of rainfall variability and it indicates the number of standard deviations that a rainfall event deviates from the average of the considered years (Funk et al. 2015). It was also used to determine the frequency of dry and wet years in the record and used to assess the frequency and severity of droughts (Alemu and Bawoke 2019). It indicates the departure from the long-term mean with negative values representing periods of below-normal rains (droughts) while positive values reflect above normal rains (flood risk) (Muthoni et al. 2019). SAI value is classified as extremely wet (SAI > 2), very wet ($1.5 \le \mathrm{SAI} \le 1.99$), moderately wet ($1 \le \mathrm{SAI} \le 1.49$), near normal ($-0.99 \le \mathrm{SAI} \le 0.99$), moderately dry ($-1.49 \le \mathrm{SAI} \le -1$), severely dry ($-1.99 \le \mathrm{SAI} \le -1.5$) and extremely dry ($\mathrm{SAI} \le -2$) (Funk et al. 2015) and it was computed using the following equation:

$$\mathrm{SAIi} = \frac{\mathrm{Xi} - \overline{\mathrm{x}}}{\sigma} \tag{2}$$

where SAIi is the standardized anomaly index in a year i, Xi is the rainfall value in a year i; $\overline{\mathrm{x}}$ is the long-term mean of rainfall and σ is the standard deviation of rainfall.

iii. Mann-Kendall Trend Test and Sen's Slope Estimator

The study analyzed the trends and magnitudes of rainfall changes using the Mann-Kendall (MK) trend test (Non-parametric statistical test) and Sen's Slope estimator in XLSTAT 2020. MK trend test is one of the most commonly used and preferred nonparametric tests for finding trends in time series hydro-climate (Gocic and Trajkovic 2013; Ahmed et al. 2014; Feng et al. 2016). This method is less affected by missing values and uneven data distribution, and it is less sensitive to outliers because it considers ranks of the observations rather than their actual values (Kendall 1975; Poudel and Shaw 2016; Belay et al. 2019). Therefore, the World Meteorological Organization (WMO) strongly recommends the MK trend test for general use in trend analysis (Mitchell et al. 1966). It is used to confirm whether there is a statistically significant or insignificant trend in rainfall variability (Jain and Kumar 2012).

According to the MK test, the null hypothesis (H_0) of no trend, that is the observations Yi are randomly ordered in time, against the alternative hypothesis (H_1), where there is a monotonic (increasing or decreasing) trend in the time series was tested. Based on (Mann 1945; Kendall 1975; Yue et al. 2002) the MK statistics S is computed using the following formula;

$$\mathrm{S} = \sum_{\mathrm{i}=1}^{\mathrm{n}-1} \sum_{\mathrm{j}=\mathrm{i}+1}^{\mathrm{n}} \mathrm{Sign}(\mathrm{yj} - \mathrm{yi}) \tag{3}$$

where Yi and Yj are sequential data values for the time series data of length n and

$$\mathrm{Sign}(\mathrm{yj} - \mathrm{yi}) = \begin{cases} 1 & \mathrm{if}(\mathrm{yj} - \mathrm{yi}) > 0 \\ 0 & \mathrm{if}(\mathrm{yj} - \mathrm{yi}) = 0 \\ -1 & \mathrm{if}(\mathrm{yj} - \mathrm{yi}) < 0 \end{cases} \tag{4}$$

If the dataset is identically and independently distributed, then the mean of S is zero and the variance of S is given by

$$\mathrm{Var(S)} = \frac{1}{18}\left[n(n-1)(2n+5) - \sum\nolimits_{i=0}^{m} \mathrm{ti(ti-1)(2ti+5)}\right] \tag{5}$$

where n is the length of the dataset, m is the number of tied groups (a tied group is a set of sample data having the same value) in the time series and ti is the number of data points in the ith group.

The Z statistics are calculated using the formula

$$Z = \begin{cases} \frac{S+1}{\sqrt{Var(S)}} & \text{for } S < 0 \\ 0 & \text{for } S = 0 \\ \frac{S-1}{\sqrt{Var(S)}} & \text{for } S > 0 \end{cases} \quad (6)$$

A significance level $\alpha = 0.05$ was used to test either an upward or downward monotone trend. The decision for the two-tail test was made by comparing the computed Z with critical values. The null hypothesis is rejected when the absolute value of computed Z is greater than the critical values or the p-value is less than the selected significance level ($\alpha = 0.05$ or 0.1). Furthermore, when the null hypothesis is rejected, the direction of trends is upward for positive Z-value and downward for negative Z-value (Hamlaoui-Moulai et al. 2013). If the null hypothesis is rejected, the result was said to be statistically significant.

Likewise, to assess the relative strength of the MK trend test in time series data, the rate of change of the trend was determined using Sen's (1968) slope estimator. As stated by Jain and Kumar (2012), Sen's slope estimates are commonly used to determine the magnitude of trends in hydro-climate time series. It limits the influence of missing values or outliers on the slope in comparison with linear regression (Bouza-Deaño et al. 2008; Alemu and Bawoke 2019; Mekonen et al. 2020). The magnitude of the monotonic trend in hydrologic time series was calculated by using the nonparametric Sen's estimator of the slope using the following equation (Sen 1968).

$$\beta = \text{median}\left(\frac{yj - yi}{j - i}\right) \quad (7)$$

where β represents the median value of the slope values between data measurements yi and yj at the time steps i and j ($i < j$), respectively. The positive value of β indicates an increasing trend whereas the negative value of β indicates a decreasing trend. The sign of β reflects data trend direction, whereas its value indicates the steepness of the trend (Alemu and Bawoke 2019).

Correlation analysis of the Rainfall and SST

The values of r reflects the degree and direction of the relationship between two variables (Guo et al. 2014; Qian et al. 2016; Tiruneh et al. 2018). In this study, r was used to test the association between rainfall and Pacific Ocean SST. A larger absolute value of r indicates a stronger correlation between the two variables (Qian et al. 2016; Tiruneh et al. 2018). The absolute value of r was divided into a weak correlation ($0 < |r| \leqslant 0.3$), a low correlation ($0.3 < |r| \leqslant 0.5$), a moderate correlation ($0.5 < |r| \leqslant 0.8$), and a strong correlation ($0.8 < |r| \leqslant 1$) (Li et al. 2014). In the present study, r was calculated using the following equation (Mu et al. 2013).

$$r = \frac{\sum_{i=1}^{n}(Xi - \overline{X})(Yi - \overline{Y})}{\sqrt{\sum_{i=1}^{n}(Xi - \overline{X})^2 \sum_{i=1}^{n}(Yi - \overline{Y})^2}} \quad (8)$$

where r is the correlation coefficient, n is the length of the time series, and i is the number of years during the analyzed periods (1984–2018). Xi and Yi are the rainfall and the SST in the year i, respectively, and $\overline{X}$ and $\overline{Y}$ are the mean rainfall and the mean of SST, respectively during the studied periods.

Results and discussion

Validation of CHIRPS rainfall data

The results of the validation of CHIRPS rainfall data using meteorological gauge station data are presented in Table 3 at the monthly, seasonal and annual time scales. While comparison between CHIRPS and meteorological rainfall data at the monthly time scales at Asebe Teferi, Hirna, Bedesa, Gelemso, Meiso, Asebot, and Kora stations is shown in Fig. 2. The results showed a very good agreement between meteorological gauge station and CHIRPS rainfall on the monthly time scale. The r values ranges from 0.91 to 0.99, and NSE values ranges between 0.82 and 0.98 for all stations (Table 3). At the monthly basis, MAE, MBE, and RMSE values showed good performance of CHIRPS rainfall estimates in West Harerge Zone (Table 3). Monthly CHIRPS rainfall products were underestimated by about 1.2 mm, 2.5 mm, 5.3 mm, and 11.4 mm for Meiso, Hirna, Asebot, and Bedesa locations, respectively. On the other hand, monthly CHIRPS rainfall data was overestimated at Gelemso, Asebe Teferi, and Kora locations about 2.9 mm, 3.1 mm, and 10.1 mm, respectively. Based on the statistical measures, the monthly CHIRPS rainfall products perform better at Hirna and Meiso locations (Table 3) than other stations. Overall, the monthly rainfall data extracted from CHIRPS products were strongly correlated with the rainfall data for selected gauge stations. This indicates that the performance of the monthly CHIRPS rainfall product is well in the study area. This result agrees with the findings of Alemu and Bawoke (2019) in the Amhara region of Ethiopia.

Besides, CHIRPS rainfall for *Bega* (October - January) season showed good correspondence with gauge with r values ranging between 0.45 and 0.95, and NSE values between 0.21 and 0.87 for all stations. Similarly, CHIRPS rainfall data in the *Belg* season showed a very good agreement with the gauge station data with r values between 0.68 and 0.89, and NSE values ranging between 0.26 and 0.74 for all station locations. In *Kiremt* season, good agreement was observed with the gauge station data for Asebe Teferi, Bedesa, Gelemso, and Meiso station locations whereas the correlation coefficient is weak for Asebot (r = 0.26), Hirna (r = 0.32), and Kora (r = 0.36) station locations. The MAE and RMSE were small for most of the station locations relative to the gauge rainfall data in all seasons. This indicates that CHIRPS rainfall data was comparable to the gauge rainfall data in the study area. In the *Bega* season, CHIRPS rainfall data were overestimated at Asebe Teferi, Gelemso, Hirna, and Kora station locations whereas CHIRPS was underestimated at Asebot, Bedesa, and Meiso station locations in the study area. Similarly in *Belg* season, CHIRPS rainfall data were overestimated at Kora and Meiso station locations, while underestimated at Asebot, Bedesa, Asebe Teferi, Gelemso, and Hirna station locations. CHIRPS rainfall data were also overestimated at Kora and Gelemso station locations and underestimated at Asebot, Bedesa, Asebe Teferi, Meiso, and Hirna station locations during *Kiremt* season (Table 3). The result of this study is supported by the findings of Saeidizand et al. (2018) and revealed the presence of a good agreement between CHIRPS and gauge stations rainfall data in Iran during *Belg*, *Bega*, and *Kiremt* seasons.

On the annual time scale, a good agreement with the gauge station data was also observed with r values between 0.56 and 0.81 and NSE values between 0.04 and 0.59 for all station locations, except Asebot (r = 0.37) and Hirna (r = 0.4). The MBE, MAE, and RMSE for Asebot and Hirna station locations were small relative to the gauge station rainfall (Table 3) and it was comparable to the gauge station data in the study area. On the annual time scale, CHIRPS rainfall data were underestimated at Asebot, Bedesa, Asebe Teferi, Meiso, and at Hirna station locations, while overestimated at Kora and Gelemso station locations. Generally, as compared to previous studies (Ayehu et al. 2018; Dinku et al. 2018; Fenta et al. 2018; Alemu and Bawoke

Table 3 Mean monthly, seasonal, and annual time scale statistical analysis of rainfall for the meteorological station and CHIRPS rainfall data

Monthly Time Scale	Asebe Teferi	Asebot	Bedessa	Gelemso	Hirna	Kora	Meiso
R	0.98	0.91	0.99	0.98	0.99	0.98	0.98
NSE	0.93	0.82	0.92	0.96	0.98	0.87	0.96
MAE	9.13	14.18	13.26	7.52	6.61	11.70	5.90
MBE	3.11	−5.31	−11.36	2.87	−2.54	10.07	−1.18
RMSE	12	20	17	12	10	15	8
Bega (October–January)							
R	0.87	0.90	0.77	0.84	0.95	0.45	0.80
NSE	0.73	0.75	0.57	0.54	0.87	0.21	0.60
MAE	10.37	8.14	13.23	9.07	5.15	9.33	10.16
MBE	3.04	−1.26	−4.34	6.12	0.53	0.17	−1.55
RMSE	13	13	17	11	6	14	15
Belg (February–May)							
R	0.68	0.77	0.89	0.83	0.84	0.72	0.84
NSE	0.45	0.55	0.74	0.68	0.69	0.26	0.68
MAE	19.10	19.31	13.49	15.74	15.68	16.28	14.37
MBE	−2.87	−5.39	−5.21	−1	−0.53	16.28	2.18
RMSE	24	25	20	20	19	28	20
Kiremt (June–September)							
R	0.63	0.26	0.61	0.88	0.33	0.37	0.53
NSE	0.31	0.02	0.08	0.727	0.04	0.07	0.25
MAE	22.25	27.63	31.91	10.38	26.80	44.05	17.37
MBE	−9.5	−9.27	−24.53	3.50	−7.62	13.75	−2.20
RMSE	29	35	36	12	38	53	22
Annual Time Scale							
R	0.56	0.37	0.68	0.81	0.395	0.568	0.689
NSE	0.29	0.021	0.035	0.594	0.017	0.092	0.46
MAE	14.74	15.747	13.16	6.202	9.601	18.855	8.689
MBE	−3.112	−5.308	−11.36	2.87	−2.539	10.066	−1.18
RMSE	17	19	17	8	13	21	11

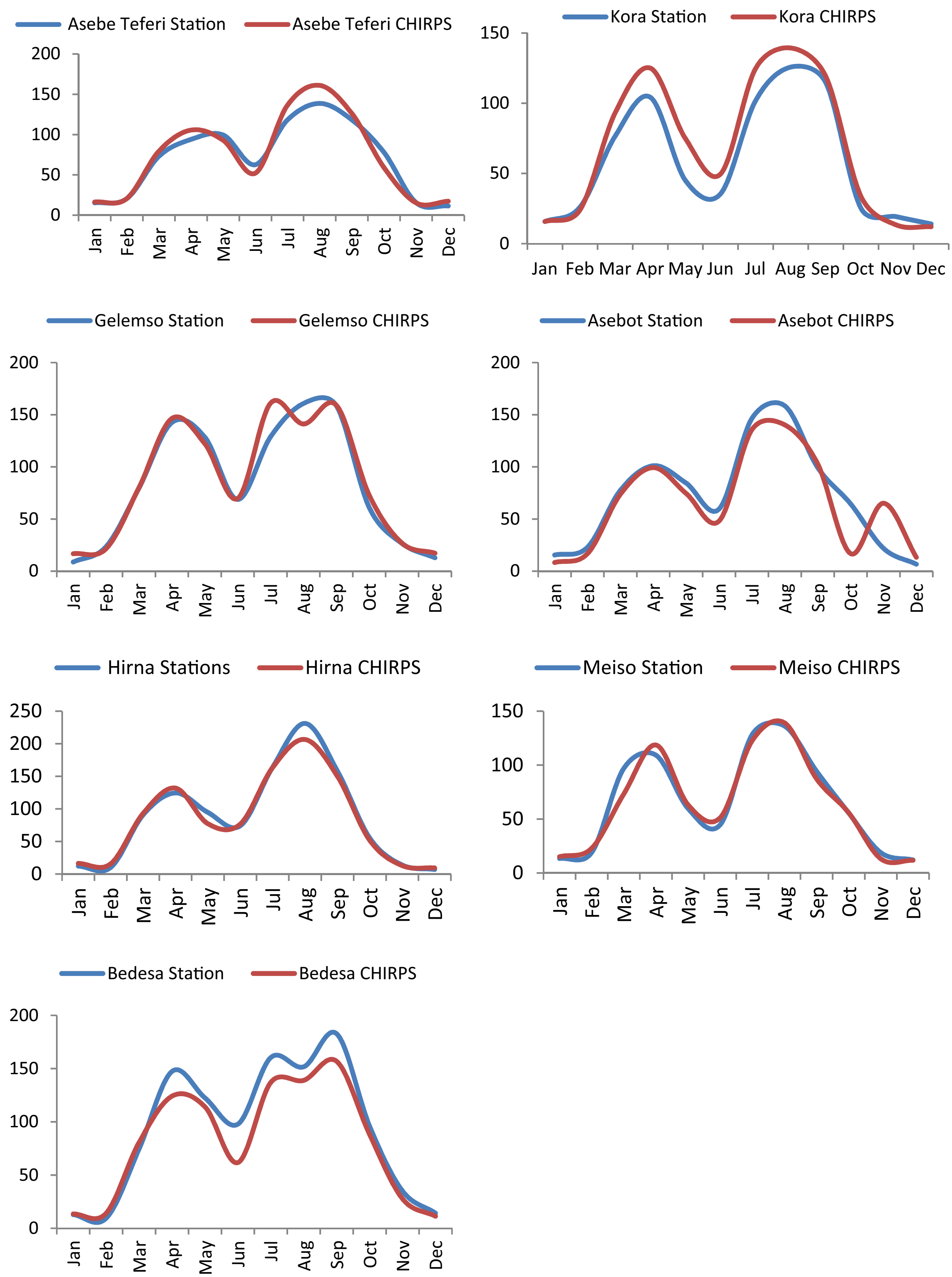

Fig. 2 Graphical comparison of mean monthly CHIRPS and meteorological station rainfall in the West Harerge Zone

2019) the CHIRPS rainfall products perform well for West Harerge Zone.

Distribution of rainfall

Long-term mean annual CHIRPS rainfall estimates (1983–2019) ranged between 528.913 and 1214.75 mm (Fig. 3b, c). This shows high spatial variability of rainfall over the area. The highest rainfall values were observed in the western, central, and northeastern parts of the study area. On the other hand, the lowest rainfall values were observed in the southeastern and northwestern parts of West Harerge Zone. The highest annual rainfall values (996–1214.75 mm) were recorded around Tulo, Goba Koricha, the northern part of Habro, the northeastern part of Mesela, southwestern part of Chiro Zuria district, the southeastern part of Anchar, and Doba district (Fig. 3b). Meiso and the southeastern part of the Boke district received the lowest annual rainfall amount (528–706 mm). The highest annual rainfall values were observed in the highest elevation area and the lowest rainfall value was recorded in the lowest elevation area (Fig. 3a, b). This result is supported by the findings of Belay et al. (2019) who reported that mean annual rainfall and elevations are highly correlated in the Beles basin of Ethiopia.

The spatial distribution of rainfall for all seasons (1983–2019) is shown below (Fig. 4a–c). During the *Bega* season, the southern and central parts of the study area received maximum rainfall value while the northern part received the lowest rainfall value. Similarly, during *Belg*, the highest rainfall values were observed in the southern, central, and northeastern parts, whereas the lowest rainfall values were recorded in northern and northwestern parts of the study area. During *Kiremt*, the highest rainfall values were recorded in the western, central, and northeastern parts while the lowest rainfall values were recorded in the southeastern and northwestern parts of the study area. *Kiremt* season rainfall was almost followed the same spatial distribution as that of the annual rainfall. Furthermore, rainfall and elevation were highly correlated in this season.

Long-term mean monthly rainfall (1983–2019) is shown in Figs. 5 and 6. It revealed that April, May, July, August, and September were the wettest months, while January, February, November, and December were the driest months. Little rainfall was recorded in March, June, and October months. The highest value of rainfall was recorded in August and September months, while the lowest value of rainfall was recorded in January month (Fig. 6). Belay et al. (2019) reported that June, July, August, and September were the main rainy months, and November, December, January, February, and March were the driest months in the Beles basin of Ethiopia.

Spatiotemporal variability and trends of rainfall in West Harerge Zone

Spatiotemporal variability of rainfall

The CV result calculated for each pixel (1983–2019) is shown in Fig. 7. Relatively highest inter-annual variability (CV > 17%) was observed in the southern, northern, and southeastern parts of the study area. In contrast, less inter-annual variability (CV < 13%) was observed in the western and northeastern parts of the area (Fig. 7). The highest inter-annual variability was experienced in the northern part of Meiso, southeastern parts of Hawi Gudina, Boke, and Kuni district, and it reflects that there is greater contrast in annual rainfall values from year to year. The majority parts of Meiso, Hawi Gudina and Boke districts experience the characteristics of lowland areas and their livelihood strategy is mainly agro-pastoralism. Due to this, their crop production potential is relatively lower as compared to highland districts of West Harerge Zone. The high inter-annual rainfall variability in these areas affects crop production, soil fertility and boost crop infestation. This situation will aggravate the reduction of crop production and food security problem. Inter-annual variability of rainfall and mean annual rainfall amounts are almost inversely related (Fig. 7). This result agrees with the findings of Dawit et al. (2019) that revealed the inverse relationship between rainfall variability and mean annual rainfall in the Guna Tana Watershed, Upper Blue Nile basin of Ethiopia. The areas with low mean annual rainfall show high inter-annual variability in the study area.

The spatial distributions of the CV of seasonal rainfall are shown below (Fig. 8a–c). As compared to annual rainfall, seasonal rainfall had high inter-annual variability up to 75.9% with *Bega* rainfall. Besides, the CV in *Kiremt* rainfall (15% < CV < 28.5%) appeared relatively stable compared to the remaining seasons. The CV of *Belg* rainfall (24% < CV < 35.58%) was higher than *Kiremt* rainfall and it indicates higher inter-annual variability of *Belg* rainfall than *Kiremt* rainfall (Fig. 8a, b). The seasonal characteristic of rainfall has a great influence on the production potential of crops in the rain-fed agricultural systems since the availability of water in the soil is essential for the growth of crops. The maximum CV in *Kiremt* rainfall was observed in the southern part of the study area. The results of this study indicate that the effect of rainfall variability on crop production and food security in the southern part is higher than other parts of the study area. On the other hand, the maximum CV in *Bega* season was observed in the northern part of the

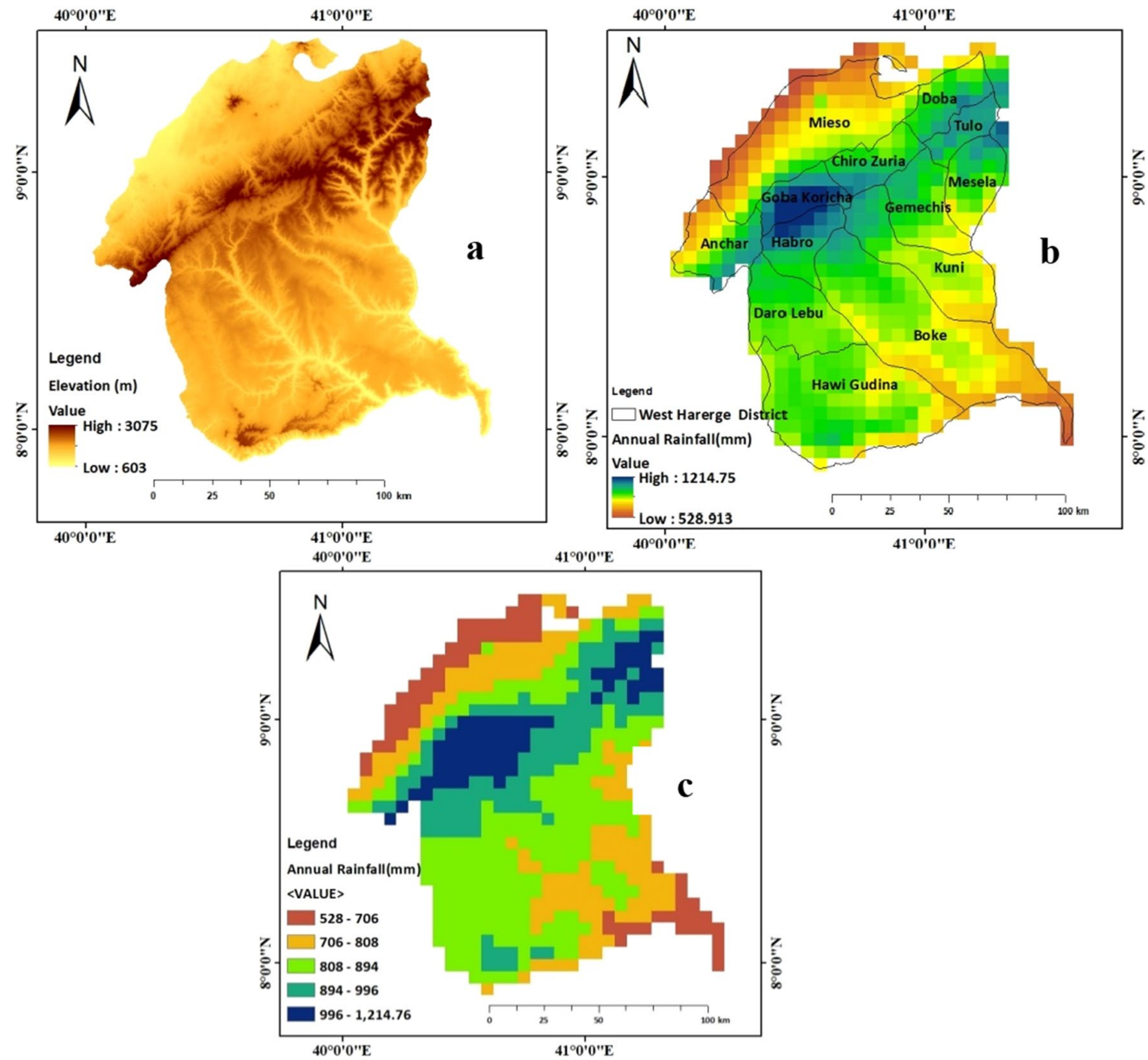

Fig. 3 Elevation (**a**), spatial distributions of long-term mean annual rainfall (mm) across the district (**b**) and spatial distributions of long-term mean annual rainfall (**c**) of West Harerge Zone (1983–2019)

study area. Similarly, the highest values of the CV in *Belg* season were recorded predominantly in the northern and southeastern parts of the study area. The result of this study agrees with the findings of Asfaw et al. (2018); Mohammed et al. (2018) and Alemu and Bawoke (2019) who reported that less variability of rainfall was observed in the *Kiremt* season than other seasons in different parts of Ethiopia.

The spatial distribution of monthly rainfall CV (%) is shown in Fig. 9. The highest inter-monthly variability (CV > 100%) was observed in January, February, October, and November months. In contrast, less inter-monthly variability (CV < 30%) was observed in some parts of the June, July, August, and September months of the study area. The result of this study agrees with the findings of Belay et al. (2019), reported a small CV in June, July, August, and September months in the Beles basin of Ethiopia.

The annual rainfall anomaly (1983–2019) over the study area is shown in Fig. 10a. The rainfall anomalies showed the presence of inter-annual variability of rainfall and the percentages of negative and positive anomalies were 56.76% and 43.24%, respectively. The highest positive anomaly (2.50) was observed in the year 1983 whereas the highest negative anomaly (2.36) was observed in the year 2015. Negative anomalies pronounced particularly in 1984, 1986–1988, 1991, 1999–2005, 2008/2009, 2011/2012, 2015/2016, and 2017 (Fig. 10a). These correspond to the historical drought years in Ethiopia due to El Niño and climate change.

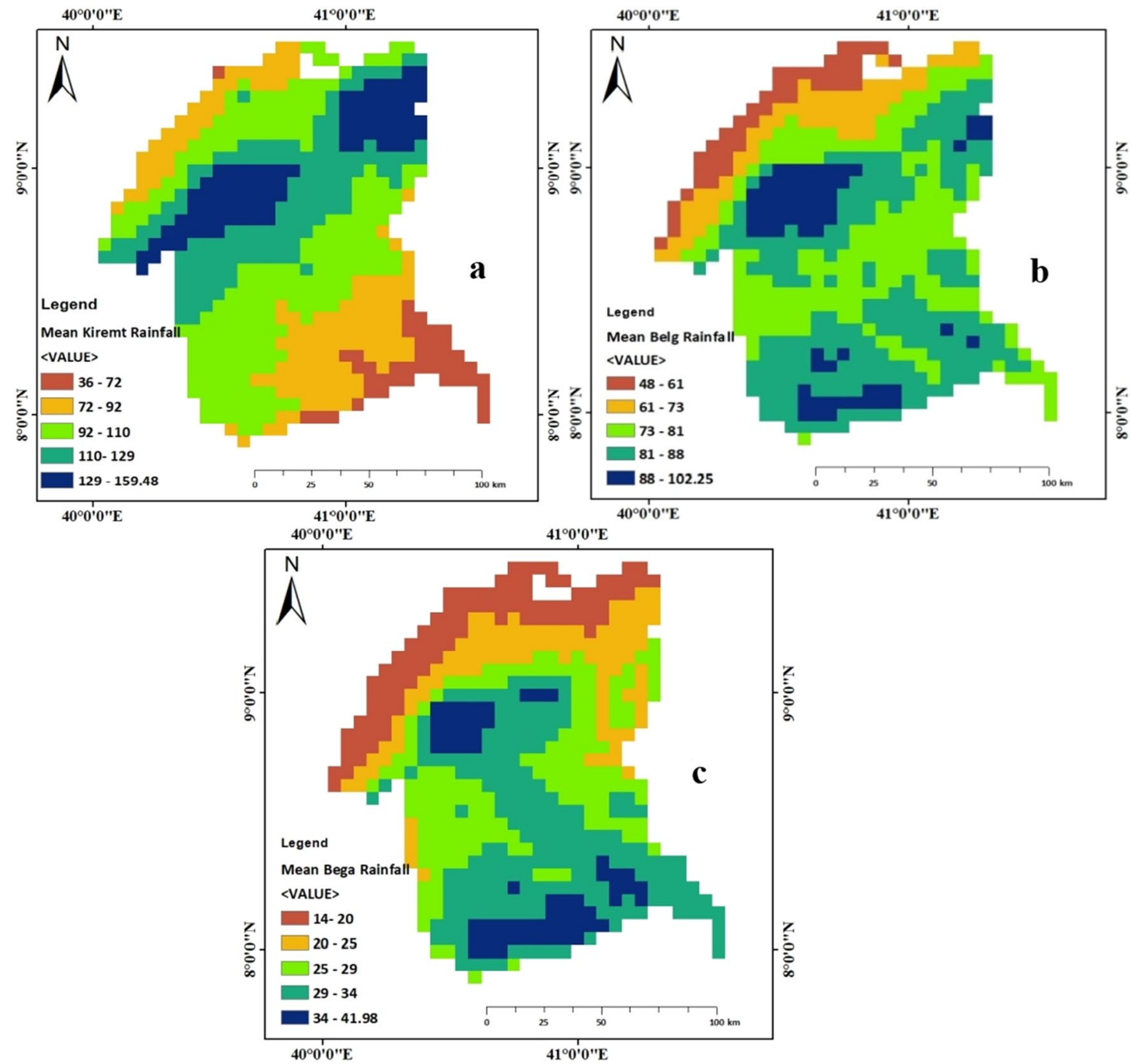

Fig. 4 Spatial distributions of mean average *Kiremt* rainfall (mm) (**a**) mean average *Belg* rainfall (mm) (**b**) and mean average *Bega* rainfall (mm) (**c**) of the West Harerge Zone (1983–2019)

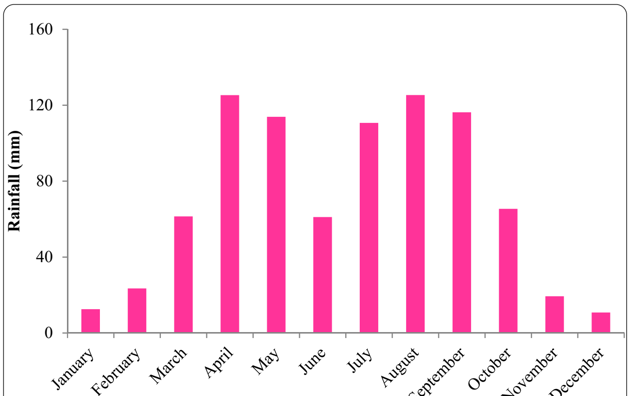

Fig. 5 Mean monthly rainfall of West Harerge Zone during 1983–2019 periods

Consequently, there was a food shortage due to reduced crop production in Ethiopia, especially in northern, central and eastern parts. This is because the majority of crop production in developing countries, including Ethiopia, depends on rain-fed agriculture. The result of this study agrees with the findings of Asfaw et al. (2018) in Ethiopia. Furthermore, the results of the SAI analysis of seasonal rainfall of the study area (1983–2019) are shown in Fig. 10b–d. The percentage of negative anomalies was larger than positive anomalies in all seasons. Similar to annual rainfall, inter-annual variability of rainfall was observed in *Belg*, *Kiremt*, and *Bega* with negative anomalies 59.46%, 54.05%, and 62.16%, respectively. The highest positive anomaly was observed in 1983, 2010, and 1997

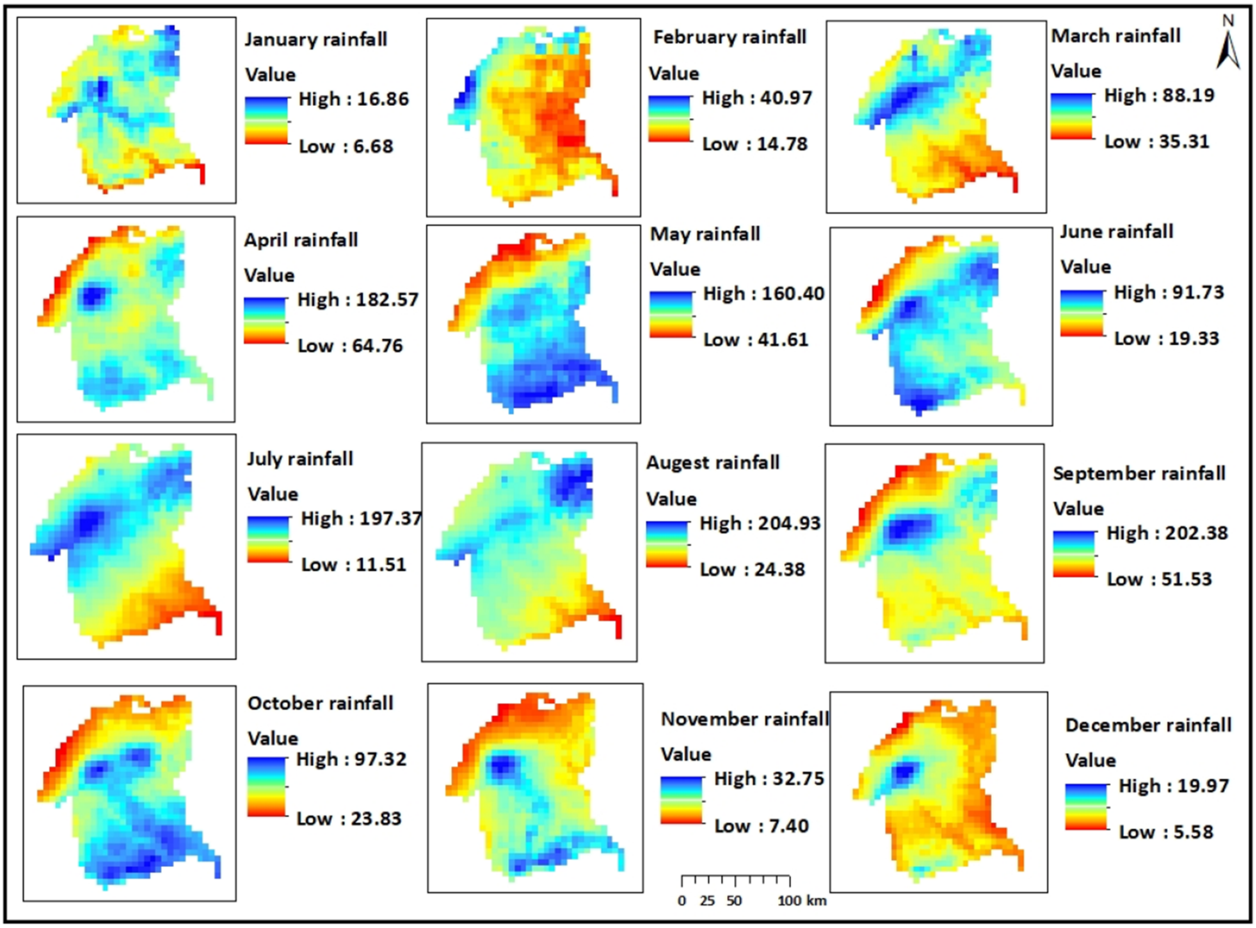

Fig. 6 Spatial distributions of mean monthly rainfall of West Harerge Zone (1983–2019)

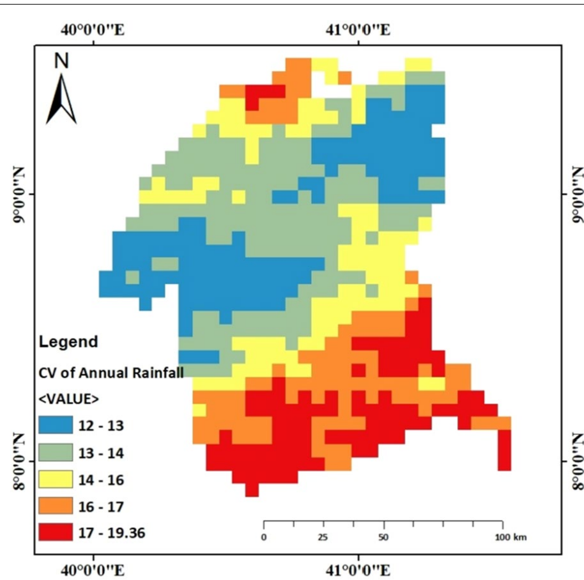

Fig. 7 Spatial distribution of CV (%) of annual rainfall in West Harerge Zone (1983–2019)

in *Kiremt*, *Belg*, and *Bega* seasons, respectively. On the other hand, the highest negative anomaly was observed in 2015, 2009, and 2010 in *Kiremt*, *Belg*, and *Bega* seasons, respectively. This result is supported by Alemu and Bawoke (2019), revealed that the percentage of negative anomalies exceeded that of positive anomalies in all seasons except *Kiremt* in the Amhara region.

Trend analysis of rainfall

The result of the monthly rainfall MK trend-test analysis is shown in Table 4. The result showed a decreasing trend of rainfall in January, February, March, April, May, June, August, September, and December months (1983–2019). On the other hand, the result of this study revealed an increasing trend in July, October, and November months (Table 4). However, the trends were not statistically significant at a significance level of $\alpha = 0.05$ in all months except November (1983–2019). The result of this study

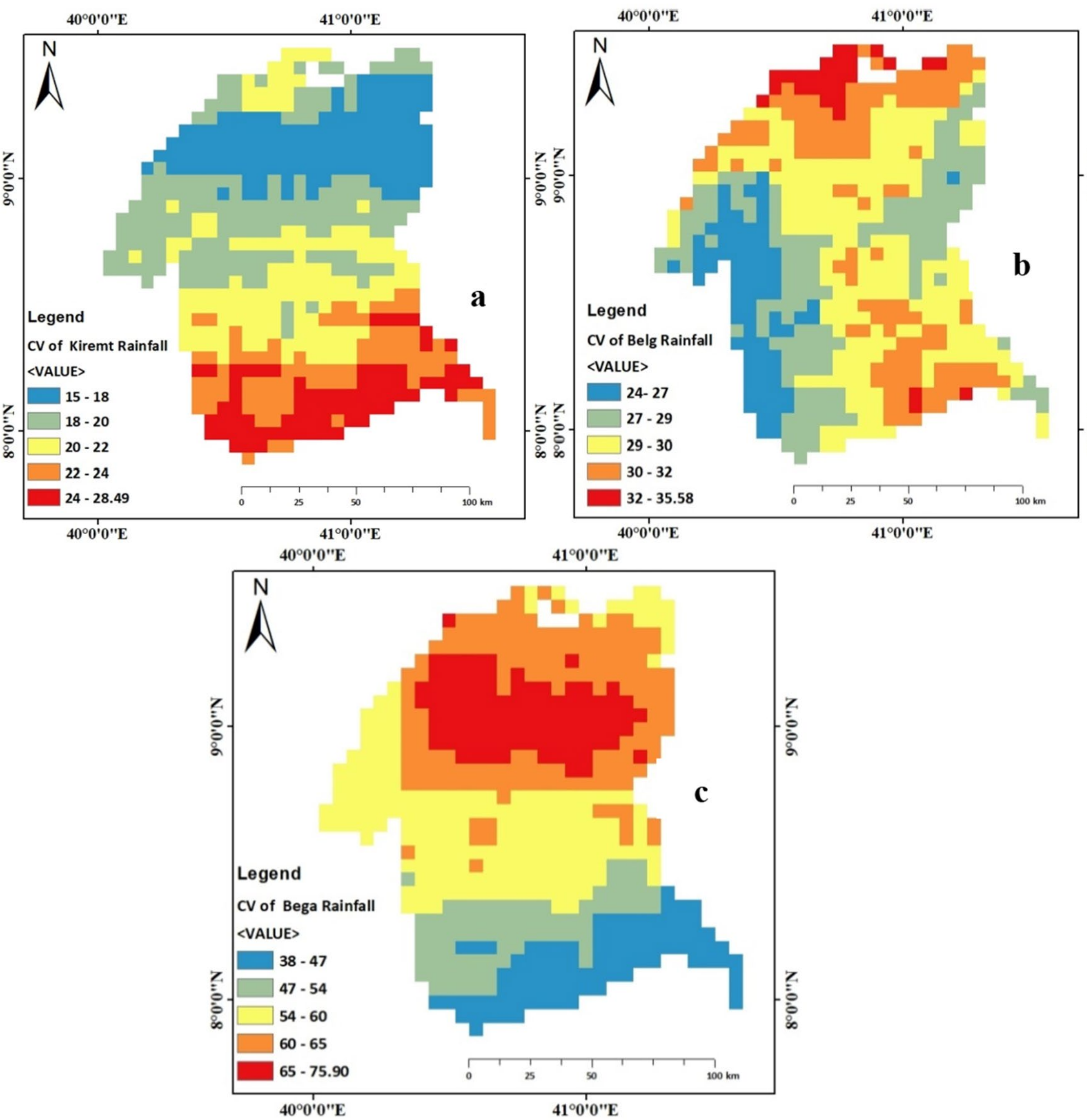

Fig. 8 Spatial distribution of CV (%) in *Kiremt* (**a**), *Belg* (**b**), and *Bega* (**c**) season rainfall in West Harerge Zone (1983–2019)

agrees with the findings of Alemu and Bawoke (2019) in the Amhara region (1981–2017).

Mean seasonal rainfall showed a downward trend in *Kiremt* and *Belg* seasons, whereas there was an upward trend in the *Bega* season (Table 5; Fig. 11b–d). The agriculture sector of most sub-Saharan countries, including Ethiopia, is predominantly rain-fed and climate-sensitive. Because of this, crop production and access to food are substantially affected by climate variability and/or climate change. The decreasing trend of rainfall in the main rainy season affects crop production and food security. The finding of this study can provide useful insight to adjust appropriate mitigation, coping and adaptation strategies by smallholder farmers. The mean seasonal rainfall was not statistically significant at $\alpha = 0.05$ in mean *Bega*, *Belg*, and *Kiremt* rainfall (1983–2019). Moreover, the mean annual rainfall showed a downward trend (Table 5; Fig. 11a) and it is not significant at a significant level of $\alpha = 0.05$. This result agrees with the findings of Viste et al. (2013) in southern Ethiopia. Mulugeta et al. (2019) also reported a non-significant decreasing trend of annual rainfall in the Awash River basin (1902–2016). In contrast, Alemu and Bawoke (2019) reported a non-significant increasing trend in the annual and *Kiremt* while a non-significant decreasing trend during the *Bega* season (1981–2017)

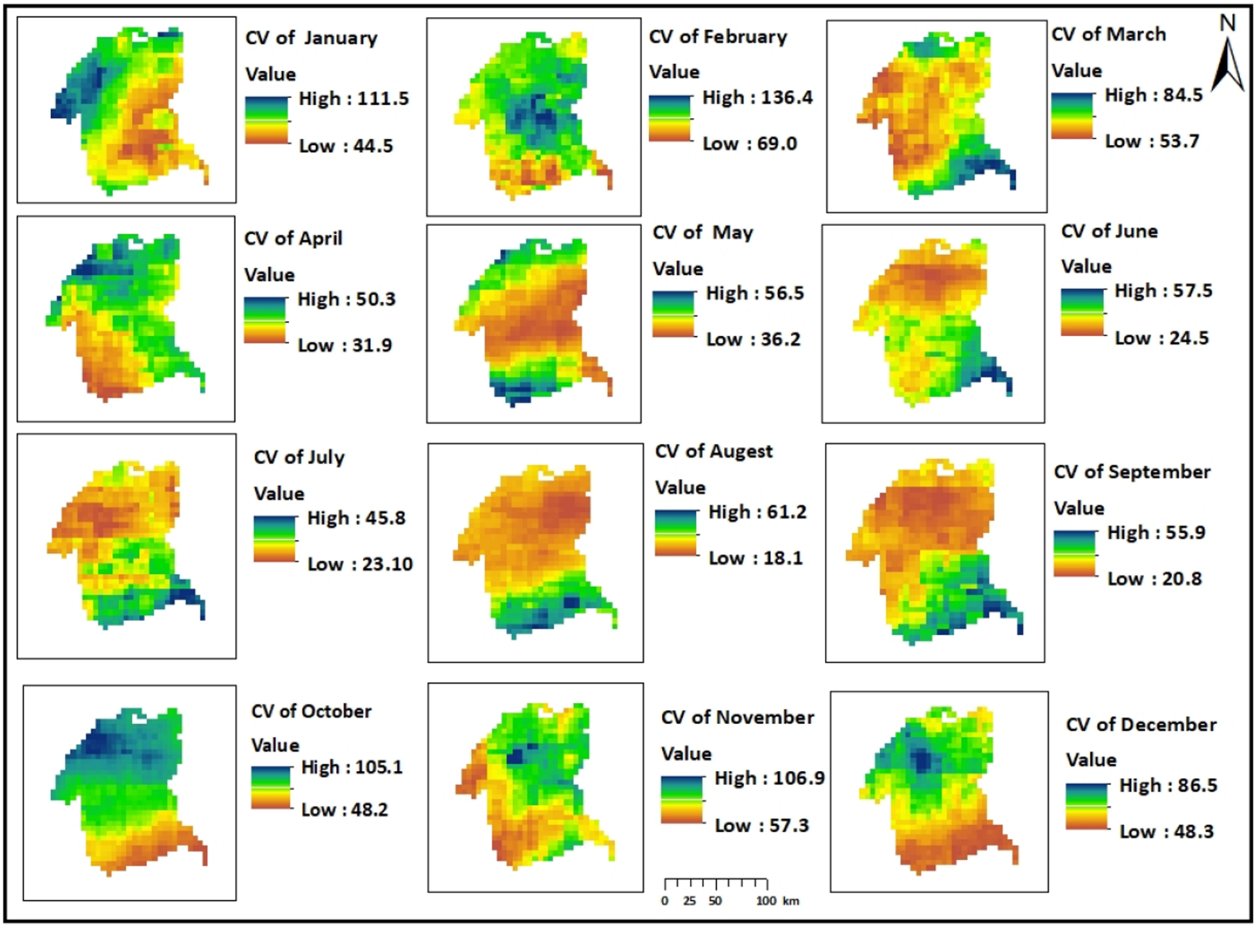

Fig. 9 Spatial distribution of monthly rainfall CV (%) of West Harerge Zone (1983–2019)

in the Amhara region of Ethiopia. The reason could be related to climate change and variability although it needs further investigation.

Associations between rainfall and Pacific Ocean Sea surface temperature (SST)

Table 6 depicts that the correlation between mean *Kiremt* rainfall and NINO 3.4 SST was negative and statistically significant (at $\alpha = 0.05$). On the other hand, the correlation between mean values of rainfall and NINO 3.4 SST was positive in *Belg* and *Bega* seasons. This implies that SST decreased the amount of rainfall in *Kiremt* season and increased in *Belg* and *Bega* seasons across the study area over the last 35 years (1984–2018). Similarly, the correlation between mean annual rainfall and NINO3.4 SST was negative in the study area. A study conducted by Tiruneh et al. (2018) revealed that the correlation between SST anomalies and rainfall was negative and positive in *Kiremt* and *Belg* seasons, respectively in the Upper Awash basin. Similarly, the negative association between mean annual rainfall and mean annual SST anomaly was reported in the Upper Awash basin. Diro et al. (2010) showed that the equatorial Pacific SST shows a negative correlation with rainfall in various parts of Ethiopia during the *Kiremt* season. Moreover, an empirical study conducted by Seleshi and Camberlin (2006) revealed that warm ENSO periods (El Niño years) are typically associated with lower rainfall and drought years. In contrast, cold periods (La Niña years) are associated with higher rainfall amounts. According to Seleshi and Camberlin (2006), the highest negative rainfall anomaly and the highest positive SST anomaly correspond to severe drought years.

The historical droughts in Ethiopia were associated with ENSO events in the past (Fekadu 2015). The drought years in Ethiopia include 1984, 1987, 1991–1992, 1993–94, 2002, 2009, 2012, 2015/16 (Asfaw et al. 2018; Mekonen et al. 2020) either coincide or follow El Niño events shortly (Asfaw et al. 2018). The finding of the present study agrees with the above result and the

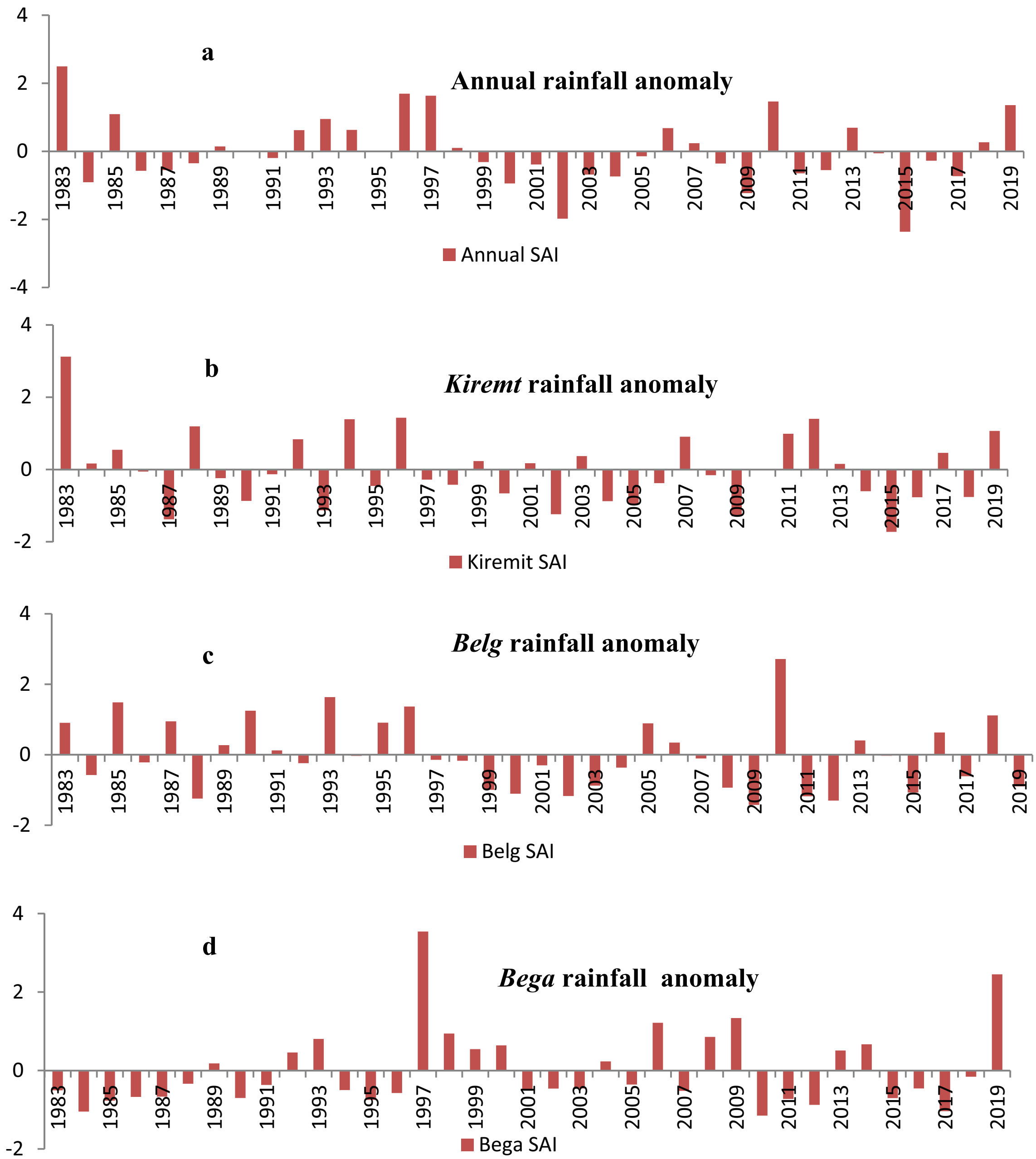

Fig. 10 Annual rainfall SAI (**a**), mean *Kiremt* rainfall SAI (**b**), mean *Belg* rainfall SAI (**c**), and mean *Bega* rainfall SAI (**d**) of West Harerge Zone (1983–2019)

rainfall anomalies for these drought periods were very low whereas the SST anomalies were very high (Fig. 12). La Nina decreases the amount of rainfall in the *Belg* season, unlike the *Kiremit* season, while El Nino increases the amount of rainfall in the *Belg* season and decreases the amount of rainfall in the *Kiremt* season (1974–2013) in Bilate River basin, Ethiopia (Moloro 2018). Besides, Yasuda et al. (2018) reported that the inter-annual variability of rainfall in East Africa was linked with the impact of Pacific Ocean SST.

Table 4 MK trend analysis of spatial average monthly rainfall in West Harerge Zone (1983–2019)

Month	Kendall's tau	S	p-value	Trend	Significance	Sen's Slope (mm/year)
January	− 0.08	− 54	0.49	Downward	Insignificant	− 0.05
February	− 0.13	− 88	0.26	Downward	Insignificant	− 0.12
March	− 0.06	− 38	0.63	Downward	Insignificant	− 0.30
April	− 0.09	− 62	0.43	Downward	Insignificant	− 0.78
May	− 0.05	− 30	0.71	Downward	Insignificant	− 0.36
June	− 0.05	− 36	0.65	Downward	Insignificant	− 0.23
July	0.01	6	0.95	Upward	Insignificant	0.01
August	− 0.07	− 46	0.56	Downward	Insignificant	− 0.32
September	− 0.06	− 38	0.63	Downward	Insignificant	− 0.20
October	0.03	20	0.81	Upward	Insignificant	0.19
November	0.35	230	0.00*	Upward	Significant	0.38
December	− 0.08	− 56	0.47	Downward	Insignificant	− 0.03

*significant at α = 0.05

Table 5 MK trend analysis of areal average annual and mean seasonal rainfall (1983–2019) in West Harerge Zone

	Kendall's tau	S	p-value	Trend	Significance	Sen's Slope (mm/year)
Annual Rainfall	− 0.09	− 62	0.43	Downward	Insignificant	− 1.46
Kiremit Rainfall	− 0.09	− 60	0.44	Downward	Insignificant	− 0.28
Belg Rainfall	− 0.18	− 122	0.11	Downward	Insignificant	− 0.61
Bega Rainfall	0.14	96	0.22	Upward	Insignificant	0.19

Conclusions

This study has investigated the spatiotemporal variability and trends of rainfall and its association with Pacific Ocean SST in West Harerge Zone of eastern Ethiopia using CHIRPS rainfall products and Pacific Ocean SST data. High spatial and temporal rainfall variability on the monthly, seasonal and annual time scales were observed across the study area. The seasonal rainfall showed high inter-annual variability in the dry season *(Bega)* than other seasons. Similarly, short rainy season (*Belg)* rainfall showed high inter-annual variability than the main rainy season (*Kiremt)*. The trends of rainfall decreased but not statistically significant in most of the months during the studied periods (1983–2019). In contrast, the trends of rainfall increased insignificantly in July and October months. However, the trend of rainfall increased significantly in November month. Besides, the trend of rainfall increased in *Bega* season and decreased in the annual, *Kiremt* and *Belg* seasons. But, the trends of rainfall were not significant at α = 0.05 significance level. Besides, NINO 3.4 SST showed a decreasing effect on the amount of rainfall in the *Kiremt* season and an increasing effect on the amount of rainfall in *Belg* and *Bega* seasons across the study area. Likewise, equatorial Pacific Ocean SST decreased the amount of rainfall in the annual time scale (1984–2018). The interaction between rainfall and Pacific Ocean SST was higher in the *Kiremt* season than *Belg* and *Bega* seasons. The Pacific Ocean SST is influenced by global warming which is caused by natural anthropogenic greenhouse gas emissions. The Pacific Ocean SST in turn affects the average rainfall amount of different parts of the world. This situation causes climate variability and/or climate change since rainfall is one of the major climate variables. Generally, the occurrence of droughts in the study area was associated with ENSO events like most other parts of Ethiopia and East Africa.

Policy implications

A very good understanding of the distribution, variability, and trend of rainfall and its association with ENSO play an indispensable role in water availability, vegetation distribution, climate change adaptation and mitigation, planning farming practice, and assessment of drought. Hence, the findings of inter-annual variability, trend, and spatial distribution of rainfall in this study should be used to develop a better decision support system in

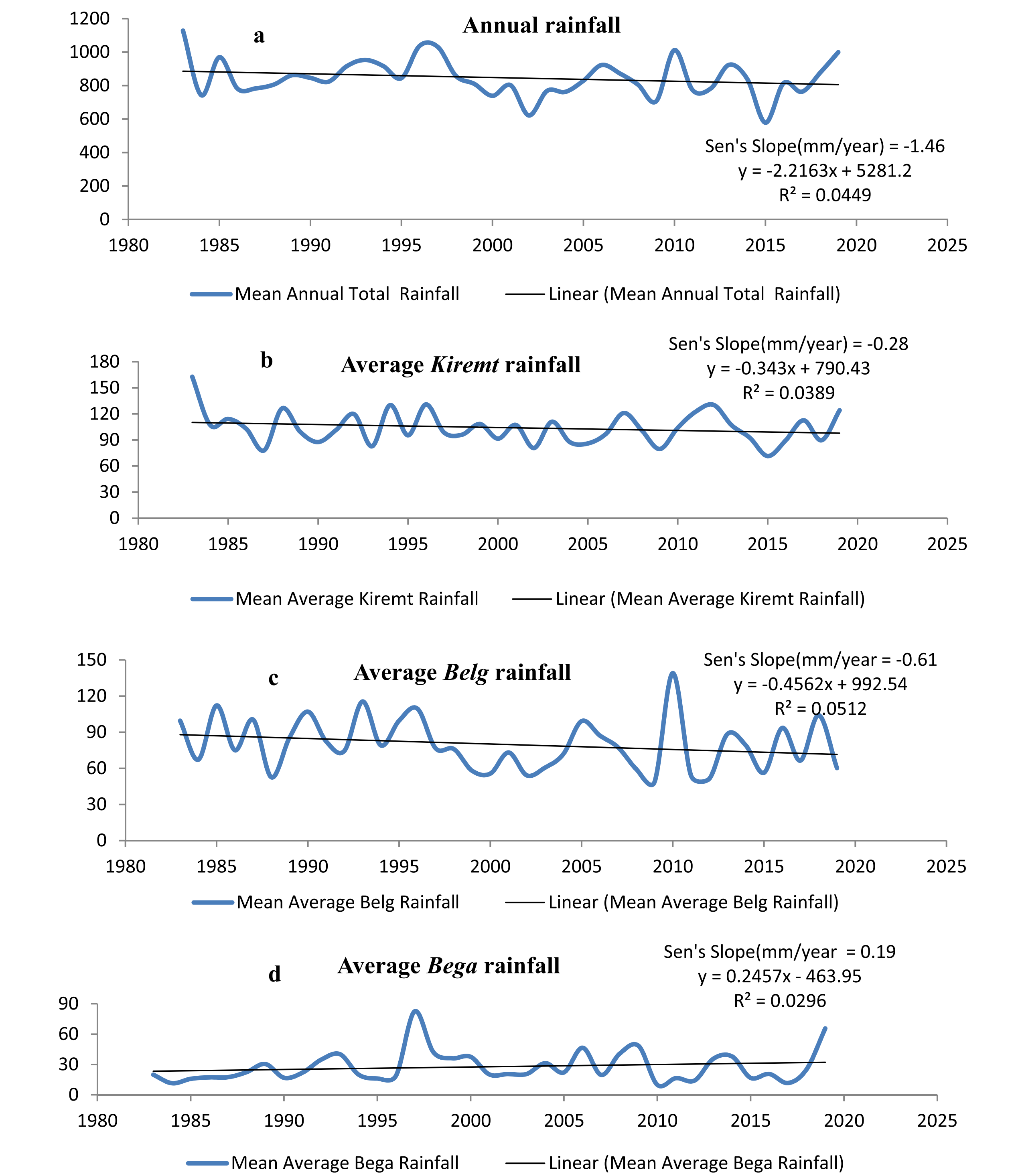

Fig. 11 Long-term annual (**a**), average *Kiremt* (**b**), *Belg* (**c**) and *Bega* (**d**) rainfall of West Harerge Zone (1983–2019)

different development activities of West Harerge Zone. It would be vital in decision support systems and preparing strategic plans to adjust sowing and planting time, select drought-resistant crops, practice in-situ water conservation, practice small-scale irrigation and diversifying incomes of smallholder farmers. Moreover, a

Table 6 Correlation coefficients between rainfall and SST (1984–2018) in West Harerge Zone

Correlation coefficients between rainfall and sea surface temperature (SST)			
	r	p-value	r^2
Kiremt	−0.46	0.01	0.21
Belg	0.27	0.18	0.05
Bega	0.25	0.14	0.06
Annual	−0.17	0.33	0.03

good understanding of rainfall is helpful in the hydrological investigation, water resource, and energy development activities. For this reason, the findings of this study should be used as a useful source of information on the spatiotemporal variability and trends of rainfall for climate risk management in and around the drought-prone regions of the study area. Moreover, effective coping and adaptation strategies should be established to combat the adverse impacts of climate change and/or variability in the study site, especially in agro-pastoralist areas. This is

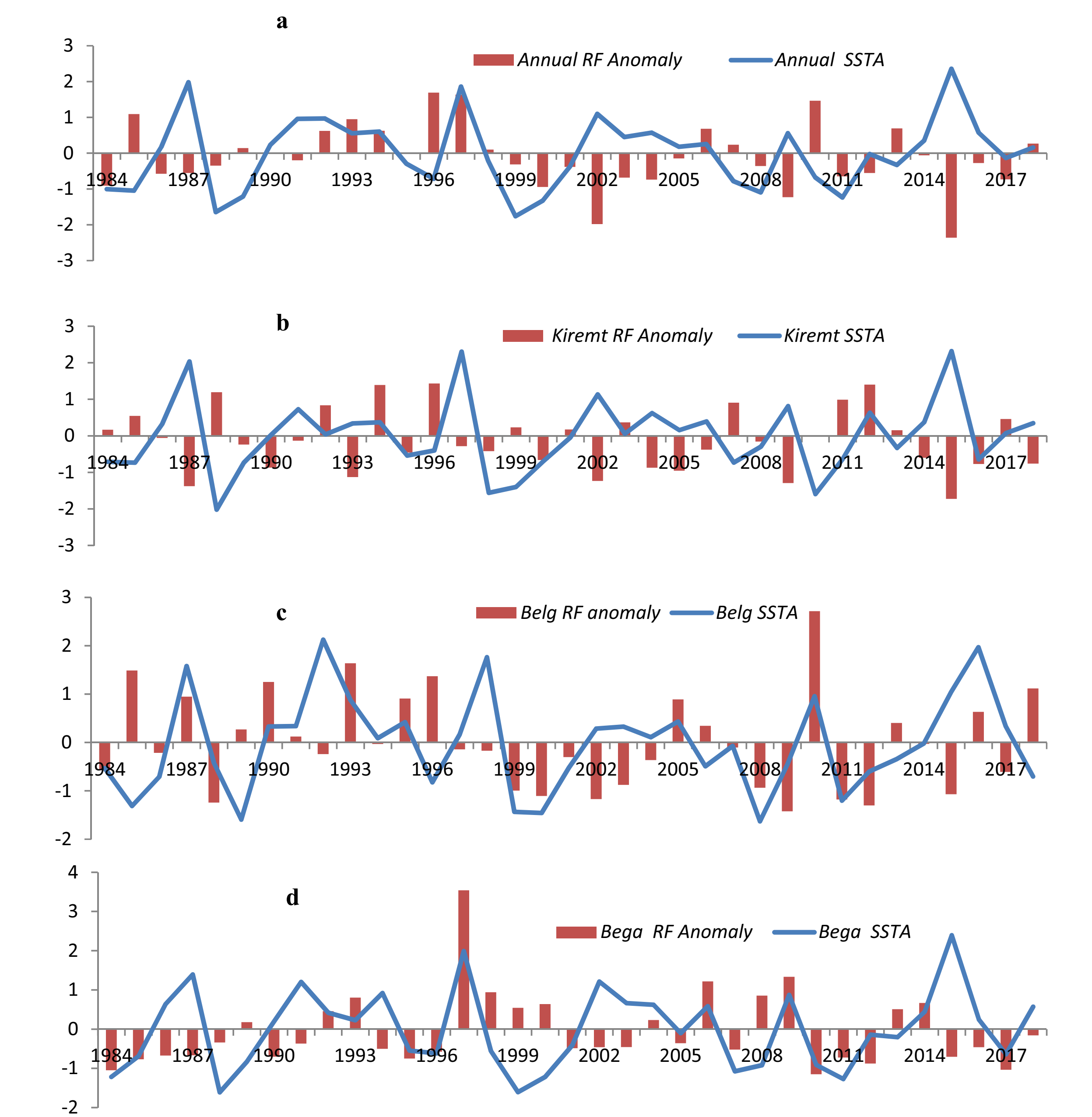

Fig. 12 Association between annual rainfall anomaly and SST anomaly (**a**), *Kiremt* rainfall anomaly and SST anomaly (**b**), *Belg* rainfall anomaly and SST anomaly (**c**) and *Bega* rainfall anomaly and SST anomaly (**d**)

because the findings of this study revealed that agro-pastoralist areas received higher spatial rainfall variability.

Abbreviations
CHIRPS: Climate Hazards Group Infra-Red Precipitation with Stations; CV: Coefficient of Variation; ENSO: El Niño/Southern Oscillation; MK: Mann-Kendall; MAE: Mean Absolute Error; MBE: Mean Bias Error; NMSA: National Meteorological Service Agency; NOAA: National Oceanic and Atmospheric Administration; NSE: Nash–Sutcliff Efficacy Coefficient; RMSE: Root Mean Square Error; r: Pearson Correlation Coefficient; SST: Sea Surface Temperature; SAI: Standardized Anomaly Index; USGS: United States Geological Survey; WMO: World Meteorological Organization.

Acknowledgements
The authors greatly acknowledge Oda Bultum University and Ethiopian National Meteorological Agency for the financial support and for providing meteorological rainfall data of the study, respectively.

Authors' contributions
All the authors had contributed to data collection and preparation, data analysis, research writing, editing. All authors read and approved the final manuscript.

Funding
The study was fully funded by Oda Bultum University.

Availability of data and materials
The data for this study can be accessed http://www.cgd.ucar.edu/cas/catalog/climind/TNI_N34/index.html and https://data.chc.ucsb.edu/products/CHIRPS-2.0/ and meteorological rainfall data is accessible in the authors' hand.

Ethics approval and consent to participate
Not applicable.

Consent for publication
Not applicable.

Competing interests
The authors declare that there are no competing interests.

Author details
[1] Department of Natural Resource Management, College of Agriculture and Environmental Science, Bahir Dar University, Bahir Dar, Ethiopia. [2] Department of Land Administration and Surveying, Institute of Land Administration, Oda Bultum University, Asebe Teferi, Ethiopia. [3] Department of Environmental Science, College of Natural Resource and Environmental Science, Oda Bultum University, Asebe Teferi, Ethiopia.

Received: 29 October 2020 Accepted: 30 December 2020
Published online: 20 January 2021

References
Abegaz WB, Mekoya A (2020) Rainfall variability and trends over Central Ethiopia. Int J Env Sci Nat Res. https://doi.org/10.19080/IJESNR.2020.24.556144
Ahmed SI, Rudra R, Dickinson T, Ahmed M (2014) Trend and periodicity of temperature time series in Ontario. Am J Clim Chang. https://doi.org/10.4236/ajcc.2014.33026
Alemu MM, Bawoke GT (2019) Analysis of spatial variability and temporal trends of rainfall in the Amhara region. Ethiopia J Water Clim Chang. https://doi.org/10.2166/wcc.2019.084
Anyah RO, Qiu W (2012) Characteristic 20th and 21st-century precipitation and temperature patterns and changes over the Greater Horn of Africa. Int J Climatol 32:347–363. https://doi.org/10.1002/joc.2270
Asfaw A, Simane B, Hassen A, Bantider A (2018) Variability and time series trend analysis of rainfall and temperature in north-central Ethiopia: A case study in Woleka sub-basin. Weather Clim Extrem 19:29–41. https://doi.org/10.1016/j.wace.2017.12.002
Ayalew D, Tesfaye K, Mamo G, Yitaferu B, Bayu W (2012) Variability of rainfall and its current trends in Amhara region, Ethiopia. Afr J Agric Res 7(10):1475–1486
Ayehu GT, Tadesse T, Gessesse B, DinkuT (2018) Validation of new satellite rainfall products over the Upper Blue Nile Basin, Ethiopia. Atmos Meas Tech 11:1921–1936. https://doi.org/10.5194/amt-11-1921-2018
Babu A (2009) The impact of Pacific sea surface temperature on the Ethiopian rainfall". Workshop on High Impact Weather Predictability Information System for Africa and AMMA THORPEX Forecasters. National Meteorological Agency, Trieste
Bayissa Y, Tadesse T, Demisse G, Shiferaw A (2017) Evaluation of satellite-based rainfall estimates and application to monitor meteorological drought for the Upper Blue Nile Basin, Ethiopia. Remote Sens. https://doi.org/10.3390/rs9070669
Belay AS, Fenta AA, Yenehun A, Nigate F, Tilahun SA, Moges MM, Dessie M, Adgo E, Nyssen J, Chen M, Van Griensven A, Walraevens K (2019) Evaluation and application of multi-source satellite rainfall product CHIRPS to assess spatiotemporal rainfall variability on data-sparse western margins of Ethiopian highlands. Remote Sens 11:1–22. https://doi.org/10.3390/rs11222688
Birkmann J, Mechler R (2015) Advancing climate adaptation and risk management. New insights, concepts, and approaches: what have we learned from the SREX and the AR5 processes? Clim Change. https://doi.org/10.1007/s10584-015-1515-y
Bouza-Deaño R, Ternero-Rodríguez M, Fernández-Espinosa AJ (2008) Trend study and assessment of surface water quality in the Ebro River (Spain). J Hydrol 361:227–239. https://doi.org/10.1016/j.jhydrol.2008.07.048
Chen Z, Wen Z, Wu R, Zhao P, Cao J (2014) Influence of two types of El Niños on the East Asian climate during boreal summer: a numerical study. Clim Dyn. https://doi.org/10.1007/s00382-013-1943-1
Cheung WH, Senay GB, Singh A (2008) Trends and spatial distribution of annual and seasonal rainfall in Ethiopia. Int J Climatol 28:1723–1734. https://doi.org/10.1002/joc.1623
Dawit M, Halefom A, Teshome A, Sisay E, Shewayirga B, Dananto M (2019) Changes and variability of precipitation and temperature in the Guna Tana watershed, Upper Blue Nile Basin, Ethiopia. Model Earth Syst Environ. https://doi.org/10.1007/s40808-019-00598-8
Degefu MA, Rowell DP, Bewket W (2017) Teleconnections between Ethiopian rainfall variability and global SSTs: observations and methods for model evaluation. Meteorol Atmos Phys 129:173–186. https://doi.org/10.1007/s00703-016-0466-9
Dinku T, Ceccato P, Grover-Kopec E, Lemma M, Connor SJ, Ropelewski CF (2007) Validation of satellite rainfall products over East Africa's complex topography. Int J Remote Sens 28:1503–1526. https://doi.org/10.1080/01431160600954688
Dinku T, Funk C, Peterson P, Maidment R, Tadesse T, Gadain H, Ceccato P (2018) Validation of the CHIRPS satellite rainfall estimates over eastern Africa. Q J R Meteorol Soc 144:292–312. https://doi.org/10.1002/qj.3244
Diro GT, Grimes DIF, Black E (2011) Teleconnections between Ethiopian summer rainfall and sea surface temperature: Part I-observation and modeling. Clim Dyn 37:103–119. https://doi.org/10.1007/s00382-010-0837-8
FAO (2019) 2018/19 El Niño High-risk countries and potential impacts on food security and agriculture
Fekadu K (2015) Ethiopian seasonal rainfall variability and prediction using Canonical Correlation Analysis (CCA). Earth Sci 4:112. https://doi.org/10.11648/j.earth.20150403.14
Feng G, Cobb S, Abdo Z, Fisher DK, Ouyang Y, Adeli A, Jenkins JN (2016) Trend analysis and forecast of precipitation, reference evapotranspiration, and rainfall deficit in the blackland prairie of eastern Mississippi. J Appl Meteorol Climatol. https://doi.org/10.1175/JAMC-D-15-0265.1
Fenta AA, Yasuda H, Shimizu K, Ibaraki Y, Haregeweyn N, Kawai T, Belay AS, Sultan D, Ebabu K (2018) Evaluation of satellite rainfall estimates over the Lake Tana basin at the source region of the Blue Nile River. Atmos Res 212:43–53. https://doi.org/10.1016/j.atmosres.2018.05.009
Funk C, Peterson P, Landsfeld M, Pedreros D, Verdin J, Shukla S, Husak G, Rowland J, Harrison L, Hoell A, Michaelsen J (2015) The climate hazards infrared precipitation with stations - A new environmental record for monitoring extremes. Sci Data. https://doi.org/10.1038/sdata.2015.66

Gebremicael T, Mohamed Y, van der Zaag P, Berhe A, Haile G, Hagos E, Hagos M (2017) Comparison and validation of eight satellite rainfall products over the rugged topography of Tekeze-Atbara Basin at different spatial and temporal scales. Hydrol Earth Syst Sci Discuss. https://doi.org/10.5194/hess-2017-504

Geremew GM, Mini S, Abegaz A (2020) Spatiotemporal variability and trends in rainfall extremes in Enebsie Sar Midir district, northwest Ethiopia. Model Earth Syst Environ 6:1177–1187. https://doi.org/10.1007/s40808-020-00749-2

Gocic M, Trajkovic S (2013) Analysis of changes in meteorological variables using Mann-Kendall and Sen's slope estimator statistical tests in Serbia. Glob Planet Change 100:172–182. https://doi.org/10.1016/j.gloplacha.2012.10.014

Goshime DW, Absi R, Ledésert B (2019) Evaluation and bias vorrection of CHIRP rainfall estimate for rainfall-runoff simulation over Lake Ziway Watershed. Ethiopia Hydrol 6:1–22. https://doi.org/10.3390/hydrology6030068

Guo W, Ni X, Jing D, Li S (2014) Spatial-temporal patterns of vegetation dynamics and their relationships to climate variations in Qinghai Lake Basin using MODIS time-series data. J Geogr Sci 24:1009–1021. https://doi.org/10.1007/s11442-014-1134-y

Hamlaoui-Moulai L, Mesbah M, Souag-Gamane D, Medjerab A (2013) Detecting hydro-climatic change using spatiotemporal analysis of rainfall time series. in Western Algeria Nat Hazards 65:1293–1311. https://doi.org/10.1007/s11069-012-0411-2

IPCC (Intergovernmental Panel on Climate Change) (2007) Climate Change 2007 - The Physical Science Basis Contribution of Working Group I to the Fourth Assessment Report of the IPCC. Cambridge University Press, Cambridge

IPCC (2014) Climate Change 2014: Mitigation of Climate Change. Summary for Policymakers and Technical Summary. In Climate Change 2014: Mitigation of Climate Change. Part of the Working Group III Contribution to the Fifth Assessment Report of the IPCC, Geneva, Switzerland. https://doi.org/10.1017/CBO9781107415416.005

IPCC (2018) Climate change 2018: impact of 1.5 °C global warming on natural and human systems [Masson-Delmottee V, Zhai P, Portner H-O, Roberts D, Skea J, Shukla PR, Pirani A, Moufouma-Okia W, Peans C, Pidcock R, Connors S, Matthews JBR, Chen Y, Zhou X, Gomis MI, Lonnoy E, Maycock T, Tignor M, Waterfeld T (eds)] (in press)

Jain SK, Kumar V (2012) Trend analysis of rainfall and temperature data for India. Current Science. 102:37-49

Jury MR, Funk C (2013) Climatic trends over Ethiopia: Regional signals and drivers. Int J Climatol 33:1924–1935. https://doi.org/10.1002/joc.3560

Katsanos D, Retalis A, Michaelides S (2016) Validation of a high-resolution precipitation database (CHIRPS) over Cyprus for a 30-year period. Atmos Res 169:459–464. https://doi.org/10.1016/j.atmosres.2015.05.015

Kendall MG (1975) Rank Correlation Methods. The Statistician 20. https://doi.org/10.2307/2986801

Kimani MW, Hoedjes JCB, Su Z (2017) An assessment of satellite-derived rainfall products relative to ground observations over East Africa. Remote Sens. https://doi.org/10.3390/rs9050430

Knapp KR, Ansari S, Bain CL, Bourassa MA, Dickinson MJ, Funk C, Helms CN, Hennon CC, Holmes CD, Huffman GJ, Kossin JP, Lee HT, Loew A, Magnusdottir G (2011) Globally gridded satellite observations for climate studies. Bull Am Meteorol Soc 92:893–907. https://doi.org/10.1175/2011BAMS3039.1

Larbi I, Hountondji FCC, Annor T, Agyare WA, Gathenya JM, Amuzu J (2018) Spatiotemporal trend analysis of rainfall and temperature extremes in the Vea catchment. Ghana Climate 6:1–17. https://doi.org/10.3390/cli6040087

Loua RT, Bencherif H, Mbatha N, Bègue N, Hauchecorne A, Bamba Z, Sivakumar V (2019) Study on temporal variations of surface temperature and rainfall at Conakry Airport, Guinea: 1960–2016. Climate 7:93. https://doi.org/10.3390/cli7070093

Mann HB (1945) Nonparametric tests against trend Econometrica 13:245. https://doi.org/10.2307/1907187

Mekasha A, Tesfaye K, Duncan AJ (2014) Trends in daily observed temperature and precipitation extremes over three Ethiopian eco-environments. Int J Climatol. https://doi.org/10.1002/joc.3816

Mekonen AA, Berlie AB, Ferede MB (2020) Spatial and temporal drought incidence analysis in the northeastern highlands. Geoenviron Disast 7:1–7

Mengistu D, Bewket W, Lal R (2014) Recent spatiotemporal temperature and rainfall variability and trends over the Upper Blue Nile River Basin, Ethiopia. Int J Climatol 34:2278–2292. https://doi.org/10.1002/joc.3837

Mitchell JM, Dzerdzeevskii B, Flohn H, Hofmeyr WL, Lamb HH, Rao KN, Wallén CC (1966) Climatic change. WMO Technical Note, 79 (WMO-No. 195/TP. 100). World Meteorological Organization, Geneva

MOA (2000) Agro-ecological zones of Ethiopia. Ministry of Agriculture (MOA), Addis Ababa, Ethiopia. Bulletin Fuer Angewandte Geologie. https://doi.org/10.5169/seals-391142

Mohammed Y, Yimer F, Tadesse M, Tesfaye K (2018) Variability and trends of rainfall extreme events in the northeast highlands of Ethiopia. Int J Hydrol 2:594–605. https://doi.org/10.15406/ijh.2018.02.00131

Moloro TL (2018) Spatio-temporal analysis of rainfall variability and meteorological drought: a case study in bilate river basin, Southern Rift Valley, Ethiopia. Int J Env Sci Nat Res. https://doi.org/10.19080/IJESNR.2018.14.555891

Mu S, Yang H, Li J, Chen Y, Gang C, Zhou W, Ju W (2013) Spatio-temporal dynamics of vegetation coverage and its relationship with climate factors in Inner Mongolia, China. J Geogr Sci 23:231–246. https://doi.org/10.1007/s11442-013-1006-x

Mulugeta S, Fedler C, Ayana M (2019) Analysis of long-term trends of annual and seasonal rainfall in the Awash River Basin, Ethiopia. Water (Switzerland) 11. https://doi.org/10.3390/w11071498

Muthoni FK, Odongo VO, Ochieng J, Mugalavai EM, Mourice SK, Hoesche-Zeledon I, Mwila M, Bekunda M (2019) Long-term spatial-temporal trends and variability of rainfall over Eastern and Southern Africa. Theor Appl Climatol 137:1869–1882. https://doi.org/10.1007/s00704-018-2712-1

Nash JE, Sutcliffe JV (1970) River flow forecasting through conceptual models part I-a discussion of principles. J Hydrol 10:282–290. https://doi.org/10.1016/0022-1694(70)90255-6

Nogueira SMC, Moreira MA, Volpato MML (2018) Evaluating precipitation estimates from Eta, TRMM and CHRIPS data in the south-southeast region of Minas Gerais state-Brazil. Remote Sens. https://doi.org/10.3390/rs10020313

OWWDSE (2010) East Hararge and West Hararge Zone Land Use Plan Study Project: East Hararge: Arba Kurkura Sub Basin Integrated Land Use. Oromia Water Works Design and Supervision (OWWDSE), Addis Ababa, Ethiopia. 30 p.

Pal AB, Khare D, Mishra PK, Singh L (2017) Trend analysis of rainfall, temperature, and runoff data: a case study of Rangoon Watershed in Nepal. Int J Students' Res Technol Manag 5:21–38. https://doi.org/10.18510/ijsrtm.2017.535

Philip SJ (2018) Effects of Climate Change on Sea Levels and Inundation Relevant to the Pacific Islands. Science Review 43–49

Poudel S, Shaw R (2016) The relationships between climate variability and crop yield in a mountainous environment: A case study in Lamjung District. Nepal Climate. https://doi.org/10.3390/cli4010013

Qian X, Liang L, Shen Q, Sun Q, Zhang L, Liu Z, Zhao S, Qin Z (2016) Drought trends based on the VCI and its correlation with climate factors in the agricultural areas of China from 1982 to 2010. Environ Monit Assess. https://doi.org/10.1007/s10661-016-5657-9

Ratnam JV, Behera SK, MasumotoY, Yamagata T (2014) Remote effects of El Niño and Modoki events on the austral summer precipitation of Southern Africa. J Clim 27:3802–3815. https://doi.org/10.1175/JCLI-D-13-00431.1

Saeidizand R, Sabetghadam S, Tarnavsky E, Pierleoni A (2018) Evaluation of CHIRPS rainfall estimates over Iran. Q J R Meteorol Soc 144:282–291. https://doi.org/10.1002/qj.3342

Segele ZT, Lamb PJ (2005) Characterization and variability of *Kiremt* rainy season over Ethiopia. Meteorol Atmos Phys 89:153–180. https://doi.org/10.1007/s00703-005-0127-x

Seleshi Y, Camberlin P (2006) Recent changes in a dry spell and extreme rainfall events in Ethiopia. Theor Appl Climatol 83:181–191. https://doi.org/10.1007/s00704-005-0134-3

Sen PK (1968) Estimates of the regression coefficient based on Kendall's Tau. J Am Stat Assoc 63:1379–1389. https://doi.org/10.1080/01621459.1968.10480934

Tierney JE, Smerdon JE, Anchukaitis KJ, Seager R (2013) Multidecadal variability in East African hydroclimate controlled by the Indian Ocean. Nature. https://doi.org/10.1038/nature11785

Tierney JE, Ummenhofer CC, DeMenocal PB (2015) Past and future rainfall in the Horn of Africa. Sci Adv. https://doi.org/10.1126/sciadv.1500682
Tiruneh GB, Gessesse B, Besha T, Workineh G (2018) Evaluating the association between climate variability and vegetation dynamics by using remote sensing techniques: the case of Upper Awash Basin, Ethiopia. World J Agric Res 6:153–166. https://doi.org/10.12691/wjar-6-4-6
Toté C, Patricio D, Boogaard H, van der Wijngaart R, Tarnavsky E, Funk C (2015) Evaluation of satellite rainfall estimates for drought and flood monitoring in Mozambique. Remote Sens 7:1758–1776. https://doi.org/10.3390/rs70201758
Traore SS, Landmann T, Forkuo EK, Traore PCS (2014) Assessing long-term trends in vegetation productivity change over the Bani River Basin in Mali (West Africa). J Geogr Earth Sci. https://doi.org/10.15640/jges.v2n2a2
Viste E, Korecha D, Sorteberg A (2013) Recent drought and precipitation tendencies in Ethiopia. Theor Appl Climatol 112:535–551. https://doi.org/10.1007/s00704-012-0746-3
Wang Y, You W, Fan J, Jin M, Wei X, Wang Q (2018) Effects of subsequent rainfall events with different intensities on runoff and erosion in a coarse soil. Catena. https://doi.org/10.1016/j.catena.2018.06.008
Weldegerima TM, Zeleke TT, Birhanu BS, Zaitchik BF, Fetene ZA (2018) Analysis of rainfall trends and its relationship with SST signals in the Lake Tana Basin Ethiopia. Adv Meteorol. https://doi.org/10.1155/2018/5869010
Wondosen N (2017) Agricultural drought risk area assessment and mapping using Remote Sensing and GIS: a case study of west Hararge Zone, Ethiopia. Addis Ababa University
Worku LY (2015) Climate change impact on variability of rainfall intensity in the Upper Blue Nile Basin. IAHS-AISH Proceedings and Reports. https://doi.org/10.5194/piahs-366-135-2015
Worku T, Khare D, Tripathi SK (2019) Spatiotemporal trend analysis of rainfall and temperature, and its implications for crop production. J Water Clim Chang. https://doi.org/10.2166/wcc.2018.064
Wu R, Kirtman BP, Pegion K (2008) Local rainfall-SST relationship on subseasonal time scales in satellite observations and CFS. Geophys Res Lett. https://doi.org/10.1029/2008GL035883
Yasuda H, Panda SN, Abd Elbasit MAM, Kawai T, Elgamri T, Fenta AA, Nawata H (2018) Teleconnection of rainfall time series in the central Nile Basin with sea surface temperature. Paddy Water Environ 16:805–821. https://doi.org/10.1007/s10333-018-0671-x
Yin Z, Dong Q, Kong F, Cao D, Long S (2020) Seasonal and interannual variability of the Indo-Pacific Warm Pool and its associated climate factors based on remote sensing. Remote Sens. https://doi.org/10.3390/rs12071062
Yu B, Zhang X, Lin H, Yu JY (2015) Comparison of Wintertime North American climate impacts associated with multiple ENSO Indices. Atmos Ocean. https://doi.org/10.1080/07055900.2015.1079697
Yue S, Pilon P, Cavadias G (2002) Power of the Mann-Kendall and Spearman's rho tests for detecting monotonic trends in hydrological series. J Hydrol 259:254–271. https://doi.org/10.1016/S0022-1694(01)00594-7
Zaroug M (2010) The connections of Pacific SST and drought over East Africa. DEWFORA meeting at ECMWF, Improved Drought Early Warning and Forcasting to strengthen preparedness and adaptation to droughts in Africa (DEWFORA). United Kingdom 4–5 October
Zhang Q, Singh VP, Li J, Chen X (2011) Analysis of the periods of maximum consecutive wet days in China. J Geophys Res Atmos. https://doi.org/10.1029/2011JD016088
Zhao W, Yu X, Ma H, Zhu Q, Zhang Y, Qin W, Ai N, Wang Y (2015) Analysis of precipitation characteristics during 1957–2012 in the semi-arid loess Plateau, China. PLoS ONE. https://doi.org/10.1371/journal.pone.0141662

Publisher's Note